



FACULTY OF ENGINEERING AND SUSTAINABLE DEVELOPMENT  
Department of Building, Energy and Environmental Engineering

---

# Comparison of the performance of silicon and thin film solar cells at the laboratory of the University of Gävle

Author  
Cristian Baena Juan

Year 2016

Student thesis, Master degree (one year), 15 HE  
Energy Systems  
Master Programme in Energy Systems  
2015-2016

Supervisor: Björn O. Karlsson  
Examiner: Shahnaz Amiri

---



## ACKNOWLEDGEMENTS

I wanted to thank my supervisor, Björn Karlsson, for their support, dedication and knowledge throughout this master's thesis at the University of Gävle.

In the same way, to express my gratitude to the Director of the Master Program in Energy Systems, Nawzad Mardan, to allow me does the thesis in the laboratories of the Faculty of Engineering and Sustainable Development and its work throughout the year in Gävle.

Finally, in spite of remoteness, more than 3000 km away, thank to my family who supports me all the time from Spain.



## ABSTRACT

The huge environmental awareness emerging last years by reason of global warming and greenhouse effect, on one hand, and the need of finding other sources of energy production and conversion due to the declining of fossil resources and the increasing cost of this kind of energy resource, on the other hand, both have led position renewable energies as a powerful alternative on the energy production and conversion.

PV-systems have emerged at an exponential rate in recent year as the main candidate and a satisfactory possibility with respect to environmental and economic sustainability.

Nowadays, the large volume on photovoltaic market is currently dominated by four types of solar cells, divided by the semiconductor material used to absorb light and convert the energy into electricity: (1) crystalline silicon (monocrystalline and polycrystalline), (2) amorphous silicon, (3) CIGS and (4) cadmium telluride; and among them, monocrystalline silicon and CIGS technologies are installed on the building 45 of the University of Gävle, at the south face of the laboratory.

In this context and with the motivation to contribute knowledge on PV field, a comparison between single crystal solar technology and thin film CIGS technology has carried out through f ratio and performance ratio procedures in order to perform an assessment of the energy conversion of each one under field conditions.

A logger monitors the power conversion from the PV modules since June 2014 while two pyranometers monitor global and diffuse solar radiation since March 2016. It must take into account that only clear sunny days have been considered during a period from 8:00 to 14:00 in order to avoid shadows effect on the PV systems.

The results come to conclude that single crystal silicon modules present a better behavior with respect to energy conversion under no shadows effect conditions by two reason: (1) f ratio, relationship of PV conversion per kW (PV yield) between CIGS and single crystal silicon, is about 87.25% with some variations along a day due to ambient temperature, cell temperature and incidence angle; (2) PV module's performance ratio of monocrystalline silicon modules is higher than thin film CIGS ones during a sunny day about 87.56% and 76.38%, respectively; and they are consistent with usual performance ratio values between 80% and 90% since 2010 onwards.

In light of the outcome and in order to confirm these conclusions, it intends to launch a project with the objective of evaluating the data collected and compare the performance of the module after a year of measurements outdoors by the PV module's performance ratio procedure.

Along the same lines, the next step of the University of Gävle will be to launch a project with the objective of evaluating the potential to be self-sufficient.

**Keywords:**

- ✓ **SolarCellPerformance**
- ✓ **CrystallineSilicon**
- ✓ **ThinFilmCIGS**
- ✓ **EnergyConversionEfficiency**
- ✓ **PerformanceRatio**

# INDEX OF THE REPORT

1.	Introduction .....	1
1.1.	Overall overview: problem description.....	1
1.2.	Target, scope and limitations.....	3
1.3.	Disposition.....	4
2.	Background and literature survey .....	5
2.1.	Solar radiation .....	5
2.1.1.	The spectral distribution of the solar radiation .....	5
2.1.2.	Total radiation and separation of radiation.....	5
2.2.	Semiconductors.....	7
2.3.	Solar cells.....	8
2.3.1.	Operating principle .....	8
2.3.2.	Commercial solar cells technologies.....	8
2.4.	Efficiency of a PV module.....	13
2.4.1.	Definition .....	13
2.4.2.	Factors affecting energy conversion efficiency .....	15
2.4.3.	Theoretical limit: Shockley Queisser limit .....	16
2.4.4.	Experimental limit: commercial and research field.....	17
3.	Method .....	21
3.1.	Description of the experimental PV systems.....	21
3.1.1.	Location.....	21
3.1.2.	Solar panels.....	21
3.1.3.	Inverters and maximizers.....	23
3.1.4.	Pyranometers.....	23
3.2.	Procedure and operating conditions .....	24
4.	Results.....	27
5.	Discussion.....	39
6.	Conclusions .....	43
7.	References .....	45

## INDEX OF FIGURES

Fig. 2.1. Beam Normal Spectral Irradiance per wavelength before and after the influence from the atmosphere.....	5
Fig. 2.2. Different types of radiation towards a tilted surface.....	6
Fig. 2.3. Components of solar radiation.....	6
Fig. 2.4. Assembly process from a solar cell to a PV system and common components of a PV system [8].....	8
Fig 2.5. Percentage of global annual production by PV technology [9]. ....	9
Fig 2.6. Percentage of global annual production by thin film PV technology [9]. ....	9
Fig. 2.7. Silicon solar cells: a) monocrystalline silicon; b) polycrystalline silicon.....	10
Fig. 2.8. Cross section diagram of silicon solar cell technology.....	11
Fig 2.9. Cross section diagram of different thin film solar cell technologies: a) cadmium telluride; b) CIGS.....	12
Fig 2.10. Variation of STC efficiency and effective efficiency for CIGS module as a function of series resistance [4].....	14
Fig. 2.11. Affecting solar cells parameters: a) Irradiance effect; b) Cell temperature effect.....	16
Fig 2.12. PV conversion efficiency as a function of energy band gap.....	16
Fig 2.13. Efficiency comparison of technologies: best lab cells versus best lab modules [9], [21, p. 47].....	18
Fig 2.14. Conversion efficiencies of best research solar cells worldwide from 1976 through 2016 for various photovoltaic technologies. Efficiencies determined by certified agencies/laboratories. Source: National Renewable Energy Laboratory (NREL) [7], [22].	18
Fig 2.15. Conversion efficiencies of best solar cells through time for the main commercial solar cells technologies [9].....	19
Fig 2.16. Performance ratio development for PV systems [9].....	20
Fig 3.1. Basic overview of PV systems located on the laboratory of the University of Gävle .....	21
Fig 3.2. Pyranometers number 1 and number 2 placed on the laboratory system. ....	24
Fig 4.1. PV module yield as function of solar radiation for each solar cells technology: March 2016.....	27
Fig 4.2. PV module yield as function of solar radiation for each solar cells technology: April 2016.....	29
Fig 4.3. PV module yield as function of solar radiation for each solar cells technology: May 2016. ....	30
Fig 4.4. Daily solar radiation for March, April and May. ....	31
Fig 4.5. PV conversion as a function of time for each solar cells technology: a) 28/03/2016; b) 20/04/2016; c) 05/05/2016.....	32
Fig 4.6. PV yield as a function of time for each solar cells technology: a) 28/03/2016; b) 20/04/2016; c) 05/05/2016. ....	33
Fig 4.7. Ratio “f” between CIGS and mono-Si daily performance per $\text{kW}_p$ as a function of time for each solar cells technology: a) 28/03/2016; b) 20/04/2016; c) 05/05/2016 .....	34



## INDEX OF TABLES

Table 2.1. Areas for different types of solar cells technologies for obtaining 1 kW <sub>p</sub> at standard irradiance, 1 kW/m <sup>2</sup> .....	14
Table 2.2. Maximum power depending on cell temperature for each kind of technology with a temperature difference of 30 °C.....	15
Table 2.3. Confirmed terrestrial module efficiencies measured under the global AM1.5 spectrum (1000 W/m <sup>2</sup> ) at a cell temperature of 25 °C (IEC 6090-3: 2008, ASTM G-173-03 global) .....	17
Table 2.4. Summary of results for energy efficiency measurements of PV modules and electrical characteristics at STC .....	19
Table 2.5. Data of effective efficiency and module's performance ratio for Golden and Ljubljana for 0°-tilt and 30°-tilt angle. ....	20
Table 3.1. Maximum-power at Standard Testing Conditions (STC) of each PV system ....	22
Table 3.2. Electrical characteristics for each installed solar cell technology at Standard Test Conditions (STC) and Normal Operating Cell Temperature (NOCT). ....	22
Table 3.3. Mechanical specification for each installed solar cell technology.....	23
Table 4.1. Daily data and calculations of monocrystalline silicon and CIGS thin film solar cells at NOCT conditions for PV module conversion, global irradiation per square meter received, PV module yield and f ratio: March 2016 .....	27
Table 4.2. Daily data and calculations of monocrystalline silicon and CIGS thin film solar cells at NOCT conditions for PV module conversion, global irradiation per square meter received, PV module yield and f ratio: April 2016 .....	28
Table 4.3. Daily data and calculations of monocrystalline silicon and CIGS thin film solar cells at NOCT conditions for PV module conversion, global irradiation per square meter received, PV module yield and f ratio: May 2016.....	30
Table 4.4. Calculations of effective efficiency and module performance ratio: March 2016 .....	35
Table 4.5. Calculations of effective efficiency and module performance ratio: April 2016 .....	35
Table 4.6. Calculations of effective efficiency and module performance ratio: May 2016 .....	36
Table 4.7. Mean and Standard Deviation values of effective efficiency, performance ratio and f ratio: case of whole month.....	36
Table 4.8. Mean and Standard Deviation values of effective efficiency, performance ratio and f ratio: case of sunny days (highlighted in blue) .....	37
Table 4.9. Effective efficiency, performance ratio and f ratio for the best clear sunny days of each month .....	37
Table 5.1. Usual values in Gävle simulated through PVGIS database for a nominal power of the PV system of 1 kW and a 45°-tilt angle: a) Crystalline silicon; b) CIGS .....	39
Table 5.2. Usual values in Gävle simulated through PVGIS database for a nominal power of the PV system of 1 kW and a 42°-tilt angle: a) Crystalline silicon; b) CIGS .....	40



# ***REPORT***



# 1. INTRODUCTION

## 1.1. OVERALL OVERVIEW: PROBLEM DESCRIPTION

The performance of a PV-system is given by the output in kWh per installed kW during a given time period. An assessment of the efficiency under realistic conditions in the Swedish climate about CIGS thin film solar and monocrystalline silicon technology is the aim of this M.Sc. Dissertation. They are two of the leading PV market technologies.

In this day and age, the present world rate of energy consumption is alarming in view of the rapid depletion of existing conventional resources. Most energy resources come mainly from non-renewable resources such as coal, oil and natural; they are the principal fuel-based energy sources or fossil fuels.

In addition, there are two linked issues more than must be considered. On one hand, fossil fuels are the main source of pollution in the world and are the main reason of global warming. Carbon monoxide (CO), Nitrogen oxides (NO<sub>x</sub>), particulate matter or soot (PM) and unburnt hydrocarbons (HC) are the pollutants that come from the combustion of fossil fuels and must be regulated by European Union Directive. Particularly, the main reason of global warming is the increase of concentration of CO<sub>2</sub> in the atmosphere. Energy demand, on the other hand, has been increasing dramatically in the last years, much more than the population growth.

Energy usage is one of the most important concerns for the future and development of humanity. Accordingly the economic activity is strongly related with the availability of energy resources.

The rationale for the project is due to two causes:

1. The huge environmental awareness emerging last years by reason of global warming and greenhouse effect.
2. The need of finding other sources of energy production due to the lack of fossil resources and the increasing cost of this kind of energy resource.

Both causes have led position renewable energies as a powerful alternative on the energy production and conversion. Solar, wind, hydro, biomass, geothermal and ocean energy (and nuclear energy could be also included) are within these types of energy.

As the world moves onto more clean and sustainable energy options, solar energy is expected to be the main sustainable choice in order to minimize the consumption of fossil fuels and reduce worldwide total emissions of regulated pollutants that they generate during energy conversion.

There is widespread availability of resources to generate electricity from solar energy. Photovoltaic (PV) energy is expected to be the main candidate for sustainable energy production, which meets the worldwide energy demand [1].

With the declining cost of solar energy technologies and the depletion of fossil fuels; PV solar energy has emerged throughout the world at an exponential rate in recent years, offering clean, bill-free, cheaper and sustainable solutions to our energy needs [2].

The most common solar energy is photovoltaic energy because of their great advantages, which is case of this project:

- ✓ Their resources are unlimited at a human scale.
- ✓ It is very friendly with the environment.
- ✓ The maintenance is simple and inexpensive.
- ✓ Photovoltaic panels have a life expectancy up to 25 years.
- ✓ The cost decreases as technology progresses.

Conversely, the drawbacks are:

- ✓ Installation costs are high; it requires a large initial investment.
- ✓ A wide expanse of land is required to collect large-scale power.
- ✓ The aesthetics of the structures is not pleasant for users.
- ✓ Require skilled labor for installation work.
- ✓ Influence of the global solar radiation.

PV systems have been considered a satisfactory possibility with the environmental and economic sustainability. In this way, two different technologies are installed in the laboratories of University of Gävle. 9 modules are made of CIGS thin film solar cells and 24 modules are made of monocrystalline silicon solar cells, of which 18 belong to 3 common PV systems and 6 to photovoltaic tracker system. This tracker PV system is out of scope of the project. A logger monitors the power production from the PV modules which is logged every minute since June 2014. Two pyranometers monitor global and diffuse solar radiation since March 2016. These data should be used for comparison of the output of the different systems, being the aim of the project.

During the last years, several research studies have been carried out by many companies, research centers and universities in order to improve the performance of solar energy applications and the behavior of solar cells on different locations as well as new technologies and devices have come up in the photovoltaic field.

Similar comparisons have been made on these and other climatic regions of the Earth. Uppsala University conducted comparing energy production technologies for the four most important market solar cells [3]. Golden (Colorado, from United State of America) and Ljubljana (Slovenia) are cities abroad whose data of performance have been reported [4].

On the other hand, new technologies try to come up. Ubiquitous Energy, Inc. (California, from USA) has been working on Clear View Power™ technology. This is the first truly transparent solar technology, allowing any surface to convert ambient light into useful

electricity without impacting the way it looks. Two thirds of the light available for energy harvesting is in the ultraviolet and the infrared, leading to practical efficiencies over 10% while maintaining up to 90% visible transparency. This approach suffers from a tradeoff between transparency and efficiency [5].

The performance of a PV system is given by the output in kWh per installed kW during a given time period. CIGS modules need a larger area than silicon modules to give 1 kW of peak output, since the m-Si efficiency at Standard Test Conditions (STC) is higher. It is expected that the output in kWh/kW is higher for the CIGS module since its performance is less dependent of module temperature and angular of incidence than the silicon module.

## 1.2. TARGET, SCOPE AND LIMITATIONS

This M.Sc. Dissertation is part of the experimental activities carried out in the laboratory of the Faculty of Engineering and Sustainable Development in the Department of Building, Energy and Environmental Engineering at the University of Gävle. This project is being conducted in about three months and it finishes in June 2016.

The main goal of the project is the comparison of the performance between CIGS thin film solar modules and single crystal silicon modules. Thus different technologies of solar cells are compared by its electrical performance on the Sweden's weather.

In this way, the project scope includes:

1. Collection of monitored data from July 2014 to May 2016.
2. Assessment of the measures by means of data processing software.
3. An analysis of the data will be carried out and the different modules (monocrystalline silicon and CIGS thin film) will be compared in order to understand its behavior.
4. The results will be compared with the results from other scientific articles in order to compare, discuss and analyze the results.
5. A report will be written through the IMRaD structure (Introduction, Method, Results and Discussion).

The evaluation of measurements and its performance allow understand the behavior of each material and how varies on a particular location depending on several affecting parameters.

It must be stated fill factor is out of the scope. They are able to infer directly on the performance of the module as a result of total module area is not receiving the highest solar energy possible. For this case of study, fill factor is equal to unit; this means an analysis over the solar cells along period of time when shadows are not affecting on the

solar cells, from 8:00 to 14:00. In addition, don't forget tracker PV system is also out of scope of the project. To conclude, the short period of irradiance data represents a scope constraint.

### 1.3. DISPOSITION

The report of this Master thesis is structured into six chapters.

The first chapter belongs to an overview of this project, that is, some notions about the current state of energy resources and renewable energies, the rationale, target, scope and constraints of the project, the state of similar projects at this time and expected results for this case of study.

The second chapter is related the background and literature survey about the main keys of solar energy, from the sun to the Earth, description and different types of solar cells, important factors about the general behavior of PV cells such as the relationship between power and efficiency.

Once all the knowledge necessary have been explained in order to get a better understanding of the project work; the third chapter belongs to the experimental methodology where is explained, in a few words, the used experimental equipment to measure the required data as well as the operating conditions and the experimental procedure.

Results are reported in the fourth chapter for the PV yield as a function of solar radiation and PV conversion, PV yield and f ratio as a function of the time; every parameter are based on each solar cell technology type.

Assessment of PV modules results is carried out in the fifth chapter by means of a comparison with the previous summary of the current state-of-the-art of solar cell technologies displayed in the second chapter.

As a final point, after conducting researches, the sixth chapter presents the conclusions as well as possible future works are propounded.



## 2. BACKGROUND AND LITERATURE SURVEY

### 2.1. SOLAR RADIATION

#### 2.1.1. THE SPECTRAL DISTRIBUTION OF THE SOLAR RADIATION

The solar radiation towards the Earth is in an average  $1367 \text{ W/m}^2$  for a surface towards the sun outside the atmosphere. The radiation varies from the maximum value of  $1412 \text{ W/m}^2$  at New Year to about  $1322 \text{ W/m}^2$  in the beginning of July. This is due to the elliptic orbit of the Earth. The average value is  $1367 \text{ W/m}^2$ , called the solar constant, accepted by the organization "The World Radiation Center (WRC)", and has an accuracy of about 1 % [6]. The solar radiation can be divided into three parts:

1. Ultra violet radiation with wave length ( $\lambda$ ) shorter than  $0.38 \mu\text{m}$  (UV).
2. Visible light with wavelength between  $0.38$  and  $0.78 \mu\text{m}$  (VIS).
3. Infra-red radiation with wave length larger than  $0.78 \mu\text{m}$  (IR).

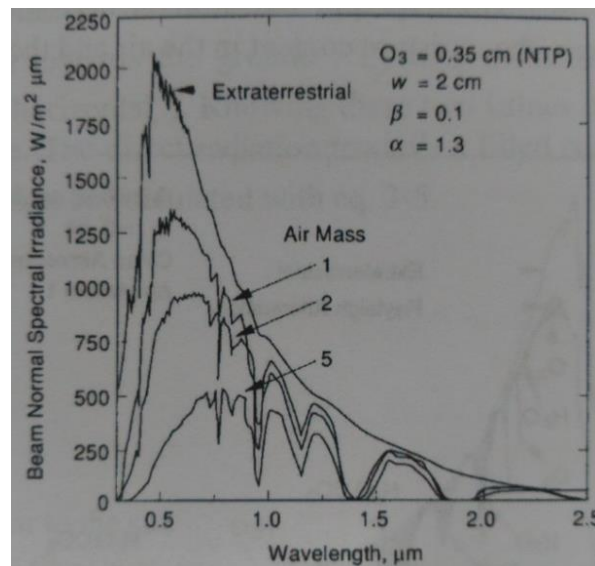


**Fig. 2.1. Beam Normal Spectral Irradiance per wavelength before and after the influence from the atmosphere.**

Spectral intensity distribution of the direct radiation before and after passing the atmosphere a clear day as a function of wavelength is displayed in Fig. 2.1. One large difference between the two curves is for wavelengths below  $0.6 \mu\text{m}$  and caused by so called Rayleigh scattering of radiation from the molecules in the air.

#### 2.1.2. TOTAL RADIATION AND SEPARATION OF RADIATION

Total radiation ( $G$ ) is the sum of the different types of radiation towards a tilted surface: beam direct radiation, diffuse radiation and ground reflected radiation.

The irradiation against a surface at the ground consists of mostly direct and diffuse radiation. The diffuse radiation is photons that have been scattered in the atmosphere.

Measurements of solar radiation is normally performed for direct radiation perpendicular to the sun,  $I_{b,n}$ , with a pyrliometer and the global total radiation towards the ground,  $I_h$ , with a horizontally tilted pyranometer. Knowing these two values the direct and the diffuse radiation can be calculated for any surface.

The distribution of the diffuse radiation from the sky is uneven, anisotropic. The distribution is more even during cloudy days, more isotropic than clear days. The diffuse radiation can roughly be divided into three parts as is displayed in Fig. 2.2.

1. Radiation from angles close to the sun, circumsolar.
2. Radiation from the bright part of the sky, just above the horizon.
3. Radiation from the rest of the sky. This part is assumed to be isotropic.

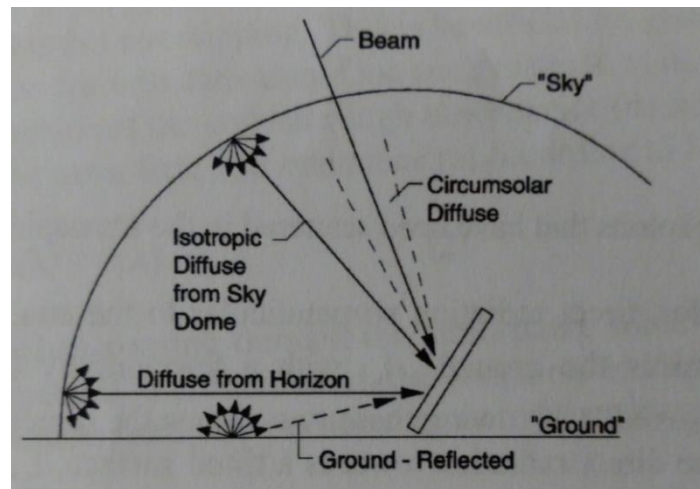


*Fig. 2.2. Different types of radiation towards a tilted surface.*

The three components of solar radiation are displayed in the Fig. 2.3. The total sum of solar radiation on a surface is named Total Solar Radiation ( $G$ ):

$$G = G_b + G_d + G_g$$

where  $G_b$  is the direct radiation towards a tilted surface,  $G_d$  is the diffuse radiation, and  $G_g$  is the ground reflected radiation.

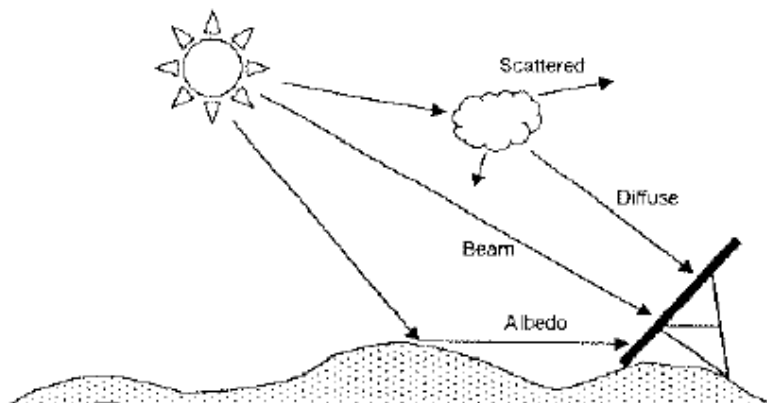


*Fig. 2.3. Components of solar radiation*

Although there are other ways such as concentrators, typically, solar energy conversion can be produced by photovoltaic or solar thermal manner. Photovoltaic cells consist of semiconductor material which is able to transform solar radiation energy into electric energy. Solar thermal devices, on the other hand, use solar radiation to produce heat.

## 2.2. SEMICONDUCTORS

Solar cells are manufactured from semiconductor materials. A semiconductor is a substance, usually a solid chemical element or compound, which acts as insulator at low temperatures but as conductor when energy or heat is available.

In other words, it is a good medium for the control of electrical current by reason of being able to conduct electricity under some conditions but not others.

Its conductance varies depending on the current or voltage applied to a control electrode, or on the intensity of irradiation by infrared (IR), visible light, ultraviolet (UV), or X rays.

The specific properties of a semiconductor depend on the impurities, or dopants, added to it. On one hand, N-type semiconductors carry current mainly in the form of negatively-charged electrons, in a manner similar to the conduction of current in a wire. Phosphorus impurities in silicon generate the N zone, which is negative. P-type semiconductors, on the other hand, carry current predominantly as electron deficiencies called holes. Boron impurities in silicon generate P zone, which is positive.

A hole has a positive electric charge, equal and opposite to the charge on an electron. In a semiconductor material, the flow of holes occurs in a direction opposite to the flow of electrons.

Currently most commercially available PV solar panels are based on inorganic semiconductors-particularly silicon, which is the second most abundant material in the earth's crust. When photons in sunlight hit a silicon solar panel, the energy frees electrons to move between dissimilar silicon crystals, generating a current of electricity. Silicon solar cells are relatively inexpensive to manufacture, but they're not the most efficient at converting solar energy into electrical energy; their maximum power conversion efficiency (PCE) appears to be 25.6 % [7].

## 2.3. SOLAR CELLS

### 2.3.1. OPERATING PRINCIPLE

A solar cell, or photovoltaic cell, is an electrical device that converts the energy of light directly into electricity by the photovoltaic effect [8].

The photoelectric effect is the phenomenon in which light particles called photons, electrons impact with a metal pulling its atoms. One of the most common applications of the photovoltaic effect is in solar cells on rooftops, converting sunlight into electricity. Because of the photovoltaic (PV) effect, two dissimilar materials in close contact produce an electrical voltage when struck by light [7].

PV panels consist of a network of photocells; common components of a PV system are displayed in Fig. 2.4.

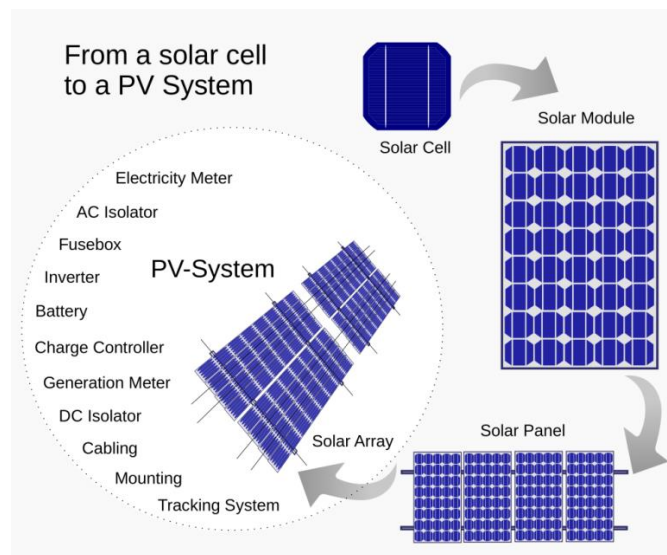


**Fig. 2.4. Assembly process from a solar cell to a PV system and common components of a PV system [8].**

### 2.3.2. COMMERCIAL SOLAR CELLS TECHNOLOGIES

Nowadays, the large volume on photovoltaic market is currently dominated by four types of solar cells, as is displayed in Fig 2.5. They are divided by the semiconductor material used to absorb light and convert the energy into electricity: (1) crystalline silicon (monocrystalline and polycrystalline both), (2) amorphous silicon, (3) CIGS and (4) cadmium telluride. The last three are within the group called thin film solar cell.

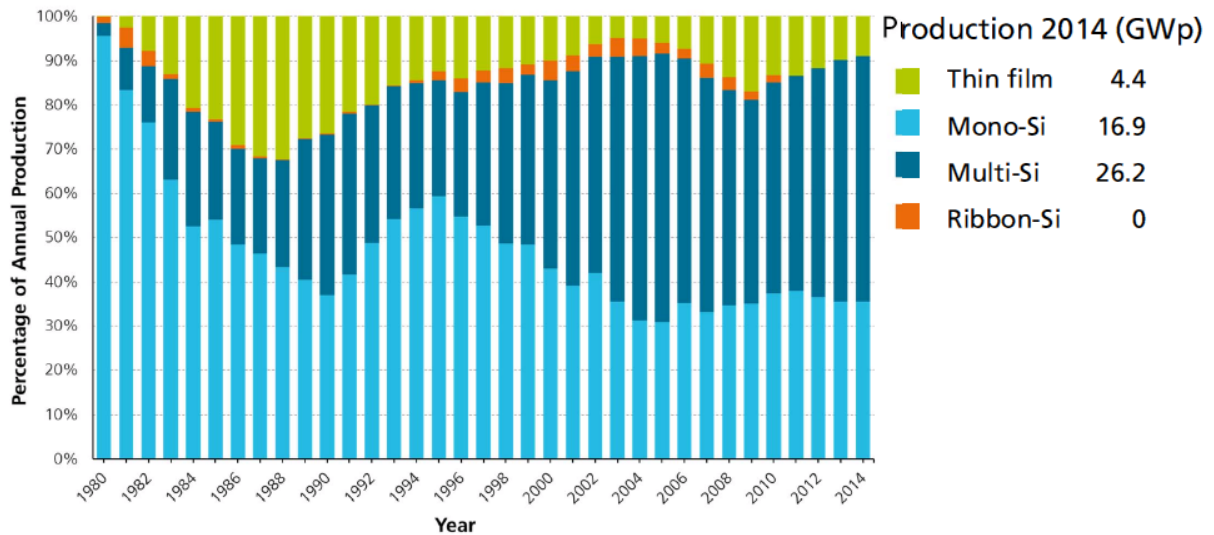


*Fig 2.5. Percentage of global annual production by PV technology [9].*

Most is still the first generation of solar cells made of crystalline silicon, both monocrystalline and multi or polycrystalline silicon, which in 2010 accounted for approximately 88% of the market [10], as is displayed in Fig 2.5.

Thin film techniques that emerged in the 1970s, also called the second generation of solar cells. They stayed in 2010 for the remaining 12% of the market, in line with Fig 2.6. Here the semiconductor material is manufactured in the form of very thin layers that is on a support material, which is mainly used glass, metal or plastic.

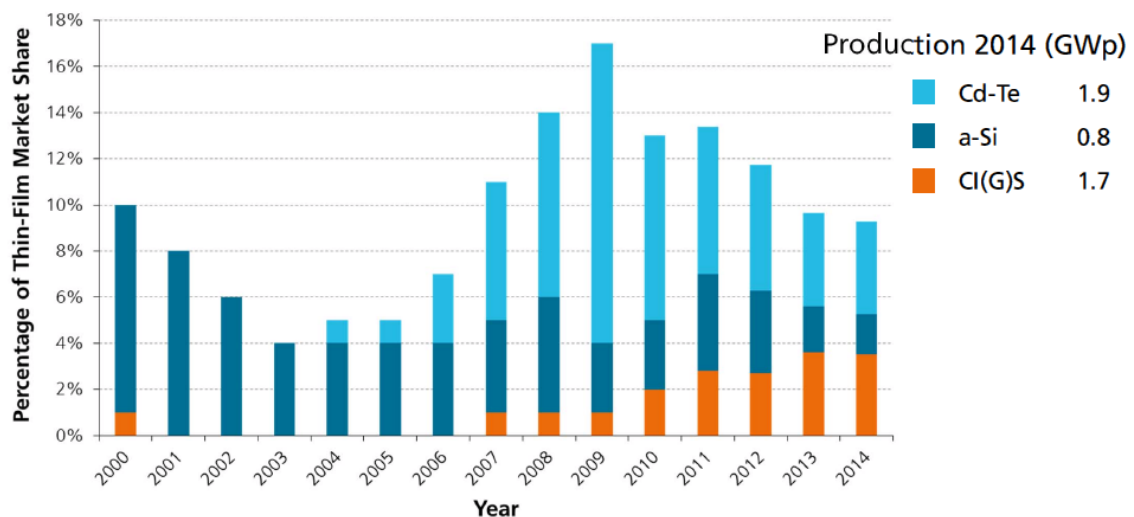


*Fig 2.6. Percentage of global annual production by thin film PV technology [9].*

Hereinafter there are classification and a description according to main solar cell technologies.

### 1. Crystalline silicon solar cells

Crystalline silicon (c-Si) is the crystalline forms of silicon, either polycrystalline silicon (p-Si) consisting of small crystals, or single crystal silicon (monocrystalline silicon, m-Si), a continuous crystal. Crystalline silicon is the dominant semiconducting material used in photovoltaic technology for the production of solar cells.

Crystalline silicon technology is the first generation of solar cells, also called, conventional, wafer-based solar cells and includes monocrystalline (m-Si) and polycrystalline (m-Si) semiconducting materials. The crystalline silicon photovoltaic modules continue to dominate the market. There are two kinds according its molecular structure, monocrystalline and polycrystalline, as it is displayed in Fig. 2.7.

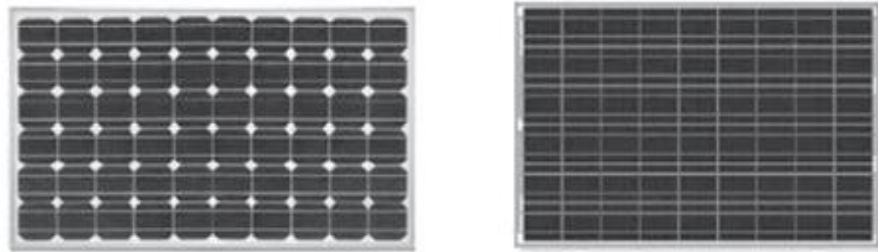


*Fig. 2.7. Silicon solar cells: a) monocrystalline silicon; b) polycrystalline silicon*

The solar cell consists of a slice of crystalline silicon. The polycrystalline silicon can be produced cheaper than the monocrystalline silicon, but is less efficient. However, polycrystalline silicon is the most commonly used material in solar cell production, giving an effective compromise between high efficiency and low material cost [11]. These silicon wafers are now between 150 microns and 250 microns thick.

As for how it is built, a PN junction is manufactured on the disc by converting the rich front of the silicon wafer typically p-type to n-type atmosphere heat treatment by phosphorus. The rear is fitted with an electrical contact of aluminum and the front pushed a fine network of leaders in a silver paste.

The individual solar cells are connected in series and then encapsulated modules. The module front panel usually consists of tempered glass, while the rear rather may consist of a special plastic wrap dense. Typically, crystalline solar modules include a plastic film on the back. A sketch of a cross section through a silicon module is displayed in Fig. 2.8.

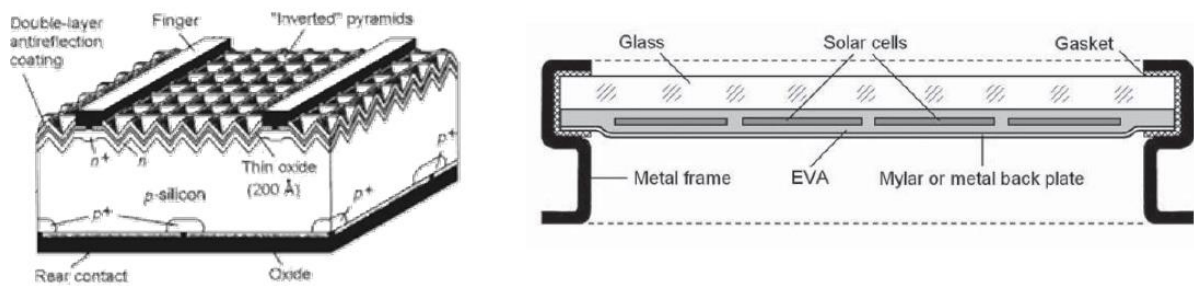


*Fig. 2.8. Cross section diagram of silicon solar cell technology*

## ❖ THIN FILM SOLAR CELLS

Thin film solar cell, also called thin film photovoltaic cell, is a solar cell that is made by depositing one or more thin layers (thin film) of photovoltaic material on a substrate [12], [13]. Thin film technologies reduce the amount of active material in a cell. Since silicon solar panels only use one pane of glass, thin film panels are approximately twice as heavy as crystalline silicon panels, although they have a smaller ecological impact (determined from life cycle analysis) [14].

This sort of solar cells has a high absorption and their thicknesses are usually between 100 and 200  $\mu\text{m}$ . Depending on the main type of material used for the absorber layer, the classification is as follows:

### 2. Amorphous silicon (a-Si)

They are the first commercial thin film solar cells and made of amorphous silicon, where the silicon atoms are not well ordered in a crystal lattice, they are in a random distribution.

In this way, silicon has a much higher absorption of light, thus, a thickness of less than 1 micron is enough for solar cell module. Typically, solar cells on amorphous silicon have considerable lower solar cell efficiency.

Since the solar cell module are often made on a glass plate in a configuration called superstrate, where the light hits the solar cell through the glass, and then come back; here consists of an opaque plastic film.



### 3. CIGS: Copper Indium Gallium (Di)Selenide ( $\text{Cu In}_x\text{Ga}_{(1-x)}\text{Se}_2$ )

CIGS photovoltaic technology is worldwide being considered as potential candidate to replace conventional Si based technology in making of solar cells. The basic components of a CIGS solar cell is the  $\text{Cu (In, Ga) Se}_2$  absorber layer, where the conversion of photons into electron-hole pairs takes place.

CIGS is an abbreviation of the chemical compound  $\text{Cu (In, Ga)}$  which is the central component of CIGS solar cells. CIGS is a semiconductor material which is especially suitable for thin film solar cells, where it is used as a thin layer with a thickness of about 2 microns. All types of thin film CIGS solar cells have reached so far the highest efficiency and therefore are considered to have the best potential in the market.

In terms of construction, CIGS thin film modules are mainly manufactured in a glass substrate in which first makes contact again directly on the glass. A glass on the front allows the passage of light in the solar cell module, while ensuring good long term stability. Fig 2.9 (b) displays a cross section diagram through a CIGS module.

### 4. Cadmium telluride (CdTe)

As in amorphous silicon modules, modules cadmium telluride may be in the superstrate configuration, and the back of the module can consist of a plastic film opaque. Since both cadmium and tellurium are toxic heavy metals, a critical aspect is to realize steady and reliable sealing modules. Most producers use a sheet of glass on the back. A cross section diagram through a CdTe module made of glass-laminated glass is displayed in Fig 2.9 (a).

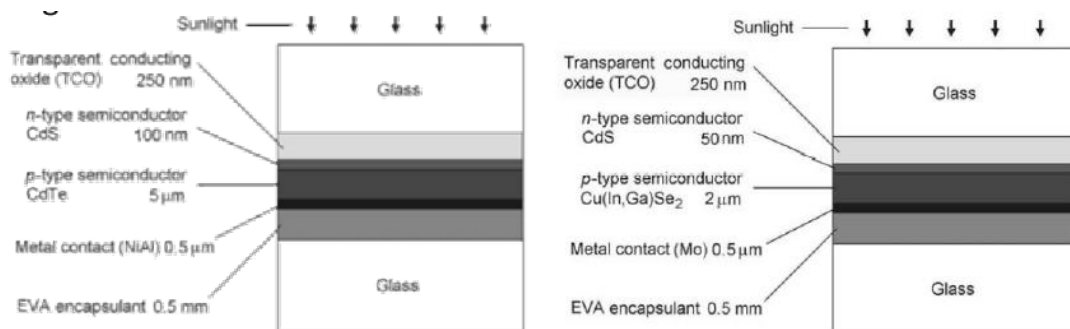


**Fig 2.9. Cross section diagram of different thin film solar cell technologies:  
a) cadmium telluride; b) CIGS**



## 2.4. EFFICIENCY OF A PV MODULE

### 2.4.1. DEFINITION

Energy conversion efficiency is measured by dividing the electrical output by the incident light power. Factors influencing output include spectral distribution, spatial distribution of power, temperature, and resistive load. IEC standard 61215 is used to compare the performance of cells and is designed around standard (terrestrial, temperate) temperature and conditions (STC): irradiance of 1 sun (1000 W/m<sup>2</sup>), a spectral distribution close to solar radiation through AM (airmass) of 1.5 and a cell temperature 25 °C. The resistive load is varied until the peak or maximum power point (MPP) is achieved. The power at this point is recorded as Watt-peak (W<sub>p</sub>). The same standard is used for measuring the power and efficiency of PV modules [15].

This means the conversion efficiency of photovoltaic modules varies with irradiance and temperature in a predictable fashion, and hence the effective efficiency averaged over a year under field conditions can be reliably assessed and determine the annual energy output of the system [4].

The efficiency ( $\eta$ ) of a cell with area A is defined as:

$$\eta = \frac{P}{G \cdot A}$$

where P is the power in W; A is the area in m<sup>2</sup>; and G is the irradiance in W/m<sup>2</sup>.

The power of a module is measured at the standard irradiance of 1000 W/m<sup>2</sup>, cell temperature of 25 °C, and normal incidence of 0°. These conditions are named Standard Test Conditions (STC), with which is obtained STC efficiency ( $\eta_{\text{STC}}$ ). This is also the maximum power in W<sub>p</sub>.

The output energy E in kWh of a module is defined as:

$$E = \eta \cdot A \cdot H = P^{\text{peak}} \cdot H$$

where A is the area in m<sup>2</sup>;  $\eta$  is the efficiency; and H is the irradiation in kWh/ m<sup>2</sup> during a period.

This means that PV systems with an equal peak power should give the same energy output. However, in practice energy output is lower than energy output at STC and is defined as:

$$E = \varphi \cdot P^{\text{peak}} \cdot H$$

where  $\varphi$  is a capacity factor, which depends on temperature of module during operation and on angle of incidence. Common values are between 0.85 and 0.9 because the operating temperature of the module is higher than 25 °C and the angle of incidence is larger than 0°. The performance at real conditions is named effective efficiency,  $\eta_{\text{eff}}$ .

Despite being an uncommon fact, capacity factor can be more than the unity, as is displayed in Fig 2.10, depending on series resistance values [4].

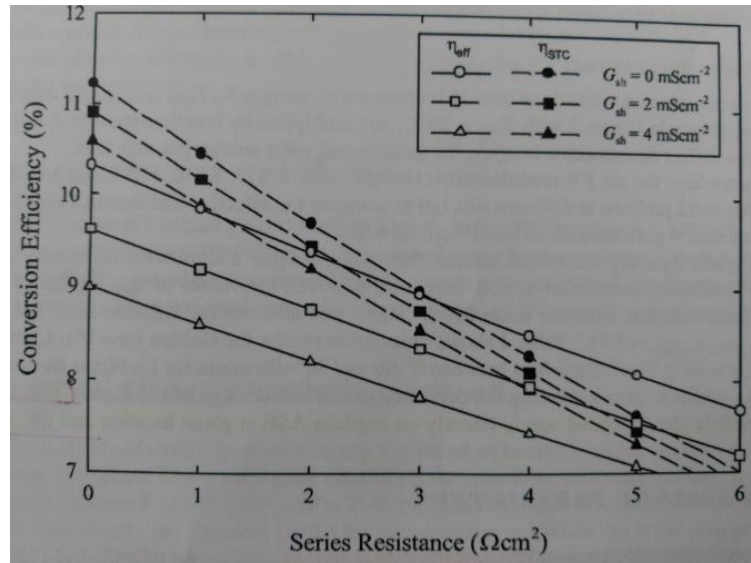


**Fig 2.10. Variation of STC efficiency and effective efficiency for CIGS module as a function of series resistance [4]**

Capacity factor is the most universal parameter for comparison of PV module outdoor performance; also known as PV module's performance ratio ( $PR_M$ ) among research community [4] is defined as the effective efficiency to STC efficiency ratio:

$$PR_M = \frac{\eta_{eff}}{\eta_{STC}} = \frac{Y_M \cdot P_0}{ASE}$$

Where  $Y_M$  is the PV module's annual yield (kWh/ yr/ kW<sub>p</sub>),  $P_0$  is the STC irradiance (1 kW/m<sup>2</sup>), and ASE is the annual solar energy per unit area (kWh/ m<sup>2</sup>/ yr).

Below is explained why CIGS modules need a larger area than Si modules to give 1 kW<sub>p</sub> of peak output, since the Si efficiency is higher. Table 2.1 displays areas for each solar cell technology at STC for obtaining 1 kW<sub>p</sub>.

$$\eta = \frac{P}{G \cdot A} = \frac{1 [kW_p]}{1 \left[ \frac{kW}{m^2} \right] \cdot A} \Rightarrow A = \frac{1}{\eta_{STC}}$$

**Table 2.1. Areas for different types of solar cells technologies for obtaining 1 kW<sub>p</sub> at standard irradiance, 1 kW/m<sup>2</sup>**

Type of solar cell	STC-Efficiency	Effective area ( $\eta \cdot A$ )	Area [m <sup>2</sup> ]
m-Si	15.27%	1 m <sup>2</sup>	6.55 m <sup>2</sup>
p-Si	13%	1 m <sup>2</sup>	7.7 m <sup>2</sup>
a-Si	6%	1 m <sup>2</sup>	16.7 m <sup>2</sup>
CIGS	≥ 11.2%	1 m <sup>2</sup>	8.93 m <sup>2</sup>

#### 2.4.2. FACTORS AFFECTING ENERGY CONVERSION EFFICIENCY

Several factors affect a cell's conversion efficiency value, including its reflectance efficiency, thermodynamic efficiency, charge carrier separation efficiency, and conduction efficiency values [15]. Because of these parameters can be difficult to measure directly, other parameters are measured instead.

The IV-curve characterizes the performance of a solar cell and a PV module. The maximum output power is given by the maximum power point MPP. The current at maximum power is called  $I_{MPP}$ , measured in amperes A. The voltage at maximum power is called  $V_{MPP}$ , measured in volts V.

$$P_{MPP} = V_{MPP} \cdot I_{MPP}$$

The maximum current is called short circuit current  $I_{SC}$ , given when voltage is equal to zero and measured in amperes A. The maximum voltage is called open circuit voltage  $V_{OC}$ , given when current is equal to zero and measured in volts V.

Accordingly, three important factors about the general behavior of solar cells are explained below:

1. The output power, that a solar cell can generate, is increasing as higher irradiance values affecting maximum power point parameter MPP; as is displayed in Fig. 2.11. (a).
2. If the cell operating temperature increases the power output will drop as is displayed in Fig. 2.11. (b). Output power varies according to temperature coefficient of  $P_{MPP}$ ,  $\gamma$ , measured in %/ °C. This parameter depends on kind of material as is displayed in Table 2.2.
3. Shadow effect is measured by the fill factor FF. Not being equally illuminated has an adverse effect on all cells' performance. An array partly shaded will not have a sufficient power output. Despite empirical formulas, the FF is most commonly determined from measurement of the IV curve and is defined as the maximum power divided by the product of  $I_{SC}$  and  $V_{OC}$ :

$$FF = \frac{I_{MPP} \cdot V_{MPP}}{I_{SC} \cdot V_{OC}}$$

**Table 2.2. Maximum power depending on cell temperature for each kind of technology with a temperature difference of 30 °C**

	m-Si	CIGS
$\gamma$	-0.44 [%/°C]	-0.38 %/°C
$P_{MPP-STC}$ (25 °C)	195 [W]	105 W
% ( $\Delta T=30$ °C)	-13.2 %	-11.4 %
$P_{MPP}$ (55 °C)	169 W	93.03 W

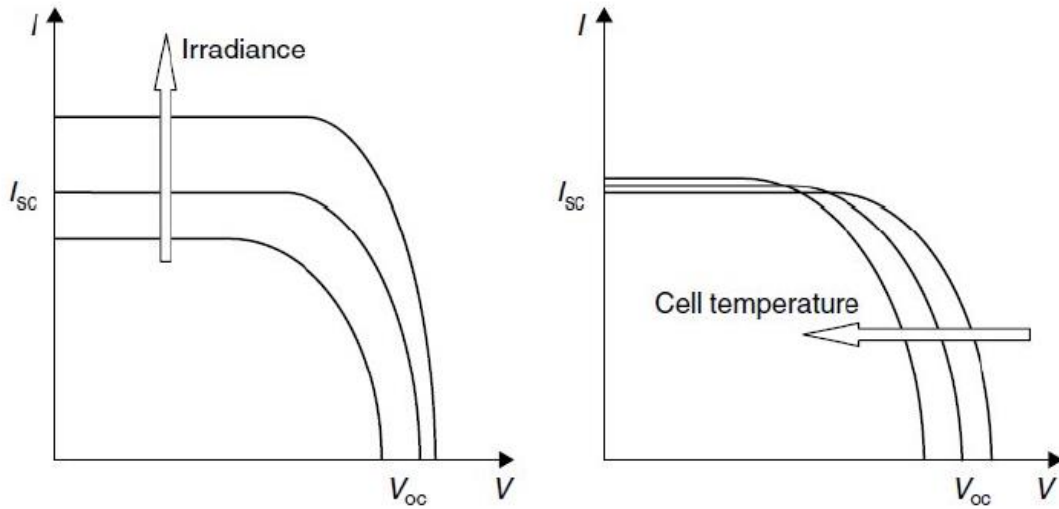


*Fig. 2.11. Affecting solar cells parameters: a) Irradiance effect; b) Cell temperature effect*

#### 2.4.3. THEORETICAL LIMIT: SHOCKLEY QUEISSER LIMIT

Shockley Queisser Efficiency Limit refers to the maximum theoretical efficiency of a solar cell using a single p-n junction to collect power from the cell.

The limit places maximum solar conversion efficiency around 33.7% assuming a single p-n junction with a band gap of 1.34 eV [16], using a cell operated at 25 °C and illuminated by the AM 1.5G spectral irradiance according to ASTM G173-03 standard, as is displayed in Fig 2.12. That is, of all the power contained in sunlight falling on an ideal solar cell (about 1000 W/m<sup>2</sup>), only 33.7% of that could ever be turned into electricity (337 W/m<sup>2</sup>). Silicon, the most popular commercial solar cell material, has a less favorable band gap of 1.1 eV. The maximum efficiency is found to be 30% for an energy gap of 1.1 eV [17], [18]. Modern commercial single crystal solar cells produce about 24% conversion efficiency, the losses due largely to practical concerns like reflection off the front surface and light blockage from the thin wires on its surface.

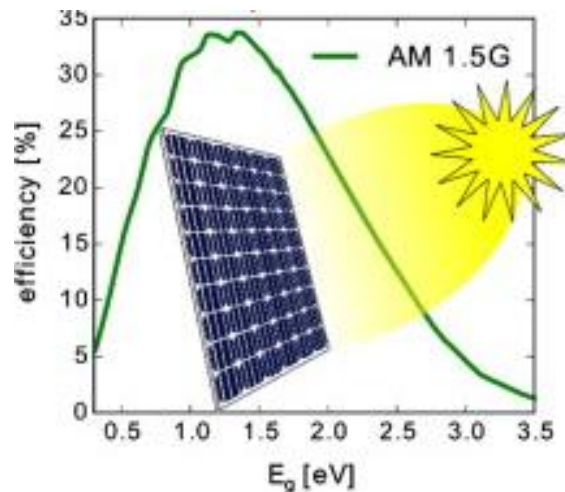


*Fig 2.12. PV conversion efficiency as a function of energy band gap*

The Shockley Queisser limit only applies to cells with a single p-n junction; cells with multiple layers can outperform this limit. In the extreme, whereas under 1 sun irradiance (1000 W/m<sup>2</sup>), a single solar cell only converts 30% of the solar energy, a tandem structure of two cells (it means two-layers cell) can reach 42%, a tandem structure of three cells can convert 49%, and a theoretical infinity-layer cell 68% in un-concentrated sunlight. Under the highest possible light concentration, these efficiencies are 40% (one-layer cell), 55% (two-layers cell), 63% (three-layers cell), and a theoretical infinity-layer cell of 68% in concentrated sunlight [19].

#### 2.4.4. EXPERIMENTAL LIMIT: COMMERCIAL AND RESEARCH FIELD.

Experimental values at Standard Test Conditions (STC) and Normal Operating Cell Temperature (NOCT) are reported in this section in order to perform a comparative analysis later in chapter number 5.

An extensive listing of the highest independently confirmed efficiencies for solar cells and modules is presented since July 2014. For a better understanding of the parameters go to Progress in Photovoltaics: Research and Applications [20].

The highest present-day confirmed terrestrial efficiencies under ASTM G-173-03 global standard is displayed in Table 2.3

**Table 2.3. Confirmed terrestrial module efficiencies measured under the global AM1.5 spectrum (1000 W/m<sup>2</sup>) at a cell temperature of 25 °C (IEC 6090-3: 2008, ASTM G-173-03 global)**

Classification <sup>a</sup>	Effic. <sup>b</sup> (%)	Area (cm <sup>2</sup> )	V <sub>oc</sub> (V)	I <sub>sc</sub> (A)	FF <sup>c</sup> (%)
Si (crystalline)	22.9±0.6	778	5.60	3.67	80.3
Si (large crystalline)	22.4±0.6	15775	69.57	6.341	80.1
Si (polycrystalline)	18.5±0.4	14661	38.97	9.149	76.2
CdTe	17.5±0.7	7021	103.1	1.553	76.6
CIGS (Cd free)	17.5±0.5	808	47.60	0.408	72.8
CIGS (thin-film)	15.7±0.5	9703	28.24	7.254	72.5
a-Si/nc-Si (tandem)	12.2±0.3	14322	202.1	1.261	68.8

<sup>a</sup>a-Si = amorphous silicon/hydrogen alloy; nc-Si = nanocrystalline or microcrystalline silicon.

<sup>b</sup>Effic. = efficiency.

<sup>c</sup>FF = fill factor.

Fig 2.13 and Fig 2.15 are reported by Fraunhofer Institute for Solar Energy Systems, ISE in Freiburg (Germany) with date of 11/03/2016 [9]. It must be stated these data (version 47) are consistent with Table 2.3 (version 45).

An efficiency comparison of each technology between best lab cells and best lab modules is displayed in Fig 2.13, while the development of Laboratory Solar Cell Efficiencies is displayed in Fig 2.15.

The record lab cell efficiency is 25.6 % for monocrystalline and 20.8 % for polycrystalline silicon wafer-based technology. The highest lab efficiency in thin film technology is 21.0 % for CdTe and 20.5 % for CIGS solar cells.

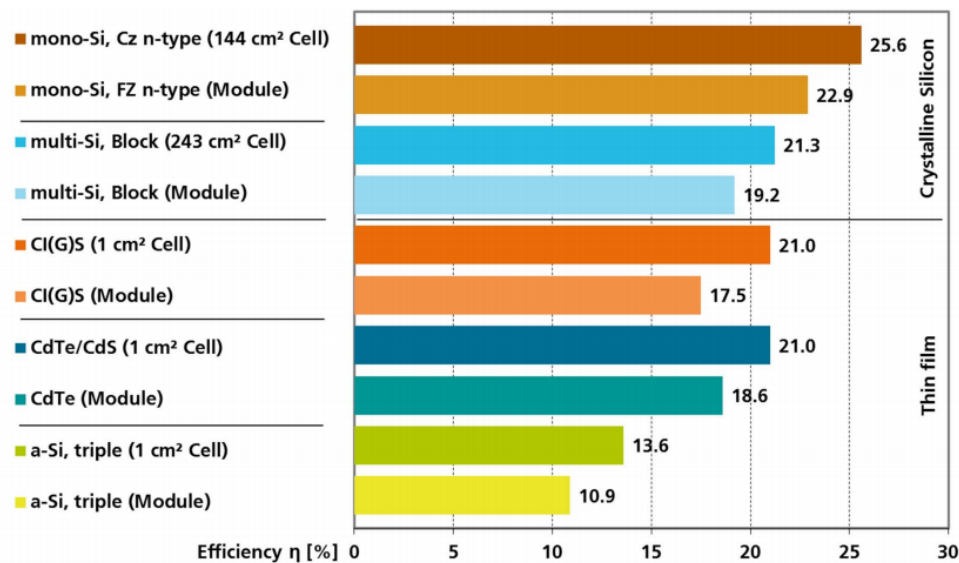


**Fig 2.13. Efficiency comparison of technologies: best lab cells versus best lab modules [9], [21, p. 47].**

In the last 10 years, the efficiency of average commercial wafer-based silicon modules increased from about 12 % to 16 %. At the same time, CdTe module efficiency increased from 9 % to 13 %.

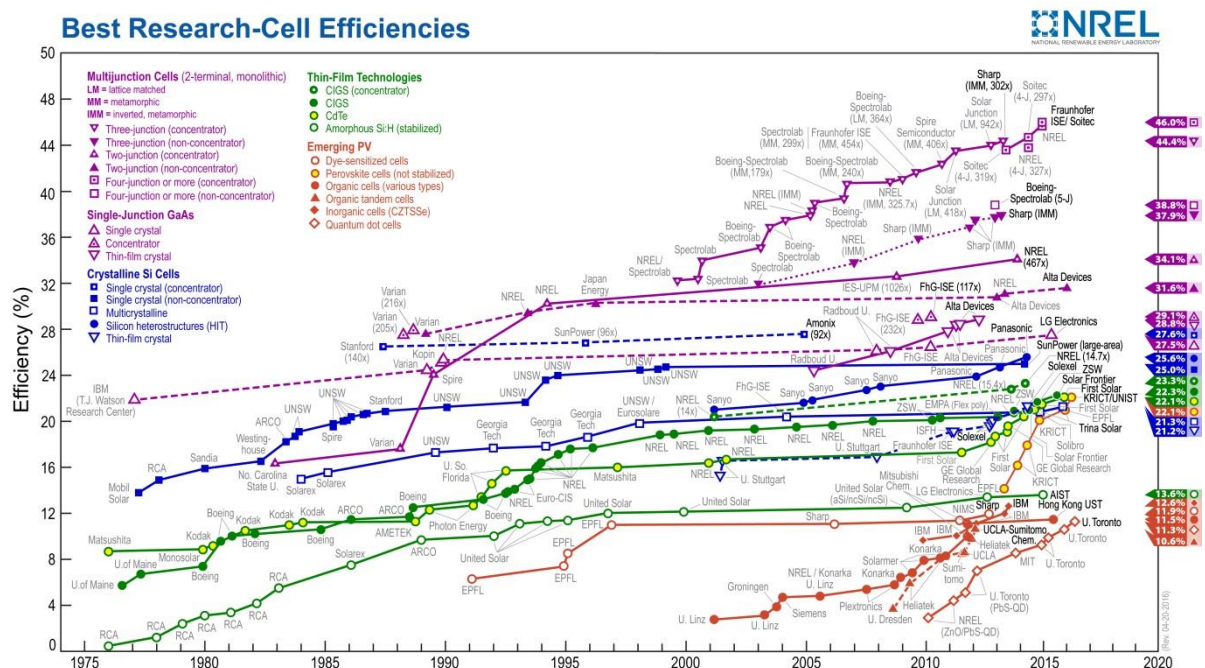


**Fig 2.14. Conversion efficiencies of best research solar cells worldwide from 1976 through 2016 for various photovoltaic technologies. Efficiencies determined by certified agencies/laboratories. Source: National Renewable Energy Laboratory (NREL) [7], [22].**



In the laboratory, best performing modules are based on monocrystalline silicon with about 23 % efficiency. Record efficiencies demonstrate the potential for further efficiency increases at the production level.

The latest chart on record cell efficiencies is displayed in Fig 2.14. Cell efficiency results are provided within different families of semiconductors: (1) multijunction cells, (2) single-junction gallium arsenide cells, (3) crystalline silicon cells, (4) thin film technologies, and (5) emerging photovoltaics. Some 26 different subcategories are indicated by distinctive colored symbols. In the same way, conversion efficiencies of best commercial solar cells are displayed in Fig 2.15.

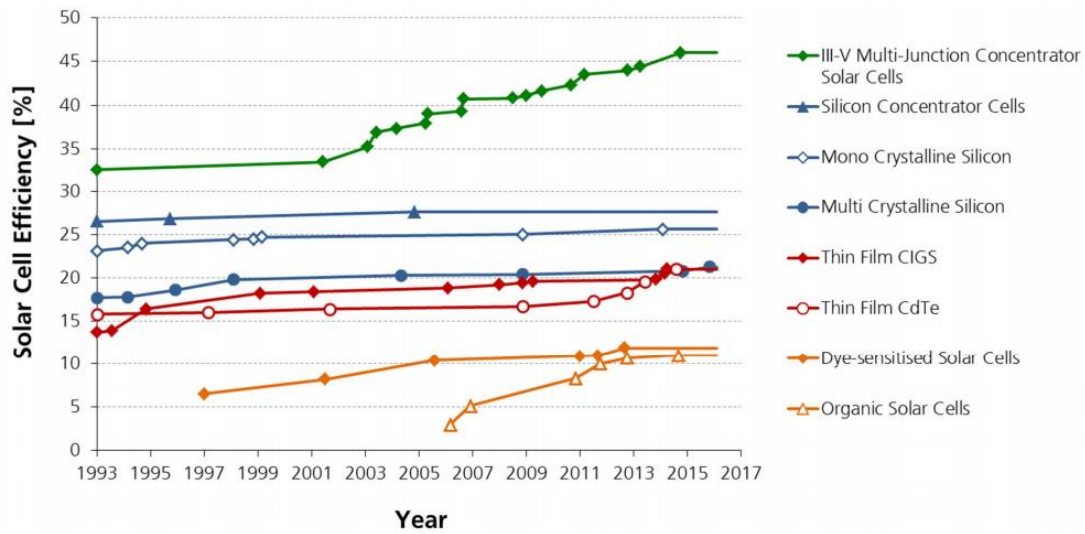


**Fig 2.15. Conversion efficiencies of best solar cells through time for the main commercial solar cells technologies [9]**

A summary of results for energy efficiency measurements of PV modules located in Uppsala (Sweden) is displayed in Table 2.4. The electrical parameters are taken from the module's own specifications according to the manufacturers' measurements at STC [3]. If CIGS module yield is divided by c-Si module yield, f ratio is equal to 0.91.

**Table 2.4. Summary of results for energy efficiency measurements of PV modules and electrical characteristics at STC**

		c-Si	a-Si	CIGS	CdTe
Area module	m <sup>2</sup>	0.68	1.43	0.75	0.72
<b>Electrical parameter</b>					
V <sub>oc</sub>	V	21.5	96.29	72.8	86.7
I <sub>sc</sub>	A	5.18	1.45	1.6	1.06
V <sub>mp</sub>	V	17.5	70.39	57.7	61.2
I <sub>mp</sub>	A	4.86	1.19	1.42	0.86
W <sub>p</sub>	W	85.05	83.76	81.93	52.63
Efficiency	%	12.45	5.86	10.93	7.31
<b>Measurement period: 2010/09/01 – 2011/08/31</b>					
Production	kWh	102.5	93.5	87.5	56.0
Yield per kWp	kWh/kW <sub>p</sub>	1206	1117	1094	1082

As regards effective efficiency and module's performance ratio, calculated results for Golden (Colorado, USA) and Ljubljana (Slovenia) are displayed in Table 2.5 for different kinds of solar cells technologies and two different tilt angles. Finally, performance ratio development as a function of annual irradiation in module plane is displayed in Fig 2.16.

*Table 2.5. Data of effective efficiency and module's performance ratio for Golden and Ljubljana for 0°-tilt and 30°-tilt angle.*

PV module	$\eta_{STC}$ (%)	Golden, Colorado ( $\phi=0^\circ$ )		Ljubljana, Slovenia ( $\phi=0^\circ$ )		Ljubljana, Slovenia ( $\phi=30^\circ$ )	
		$\eta_{eff}$ (%)	$PR_M$	$\eta_{eff}$ (%)	$PR_M$	$\eta_{eff}$ (%)	$PR_M$
SM110 (m-Si)	12.8	12.1	0.94	12.1	0.94	12.1	0.94
ASE-160 (p-Si)	11.8	10.7	0.91	10.6	0.91	10.7	0.91
WS75 (CIGS)	10.9	10.1	0.93	10.1	0.93	10.1	0.93
ST40 (CIGS)	9.6	9.0	0.94	9.1	0.95	9.0	0.95
FS55 (CdTe)	7.8	7.6	0.98	7.6	0.98	7.6	0.98
MA100 (a-Si)	6.7	6.3	0.95	6.3	0.95	6.3	0.95

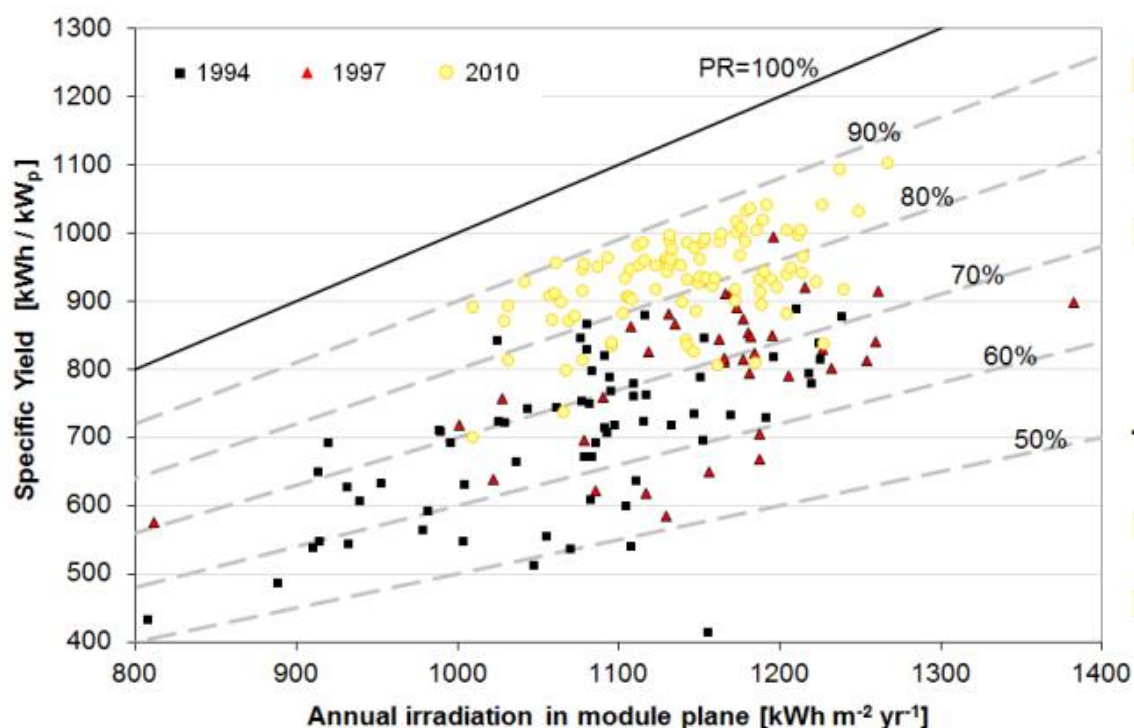


*Fig 2.16. Performance ratio development for PV systems [9]*



## 3. METHOD

### 3.1. DESCRIPTION OF THE EXPERIMENTAL PV SYSTEMS

#### 3.1.1. LOCATION

The PV modules are located in the laboratory of the Faculty of Engineering and Sustainable Development in the Department of Building, Energy and Environmental Engineering in Gävle (60° 40' 05" N, 17° 06' 48" E).

Each system consists of two identical postures and is oriented to the south with an inclination of 45°, very close to the statistically optimal slope of 42° for solar cells in Gävle. A basic overview of photovoltaic systems is displayed in Fig 3.1.



*Fig 3.1. Basic overview of PV systems located on the laboratory of the University of Gävle*

#### 3.1.2. SOLAR PANELS

The electrical system to be evaluated is a set of photovoltaic systems located in a south-facing metal structure at the laboratories of the University of Gävle.

CIGS modules and monocrystalline silicon modules are connected to an automated measurement system, constantly keeping the solar cell modules at peak power. Below is shown some data sheet values and a description of each installed systems. The maximum-power is given at Standard Testing Conditions (STC), shown in Table 3.1.

**Table 3.1. Maximum-power at Standard Testing Conditions (STC) of each PV system**

	CIGS	m-Si	m-Si (tracker)
<b>Nº PV-systems (<math>\approx 1 \text{ kW}_p</math>)</b>	1	3	1
<b>Nº modules per PV-system</b>	9	6	6
<b>Max-power per module [W]</b>	105	195	195
<b>Max-power per PV system [W]</b>	<b>945</b>	<b>1170</b>	<b>1170</b>
<b>Total max-power [W]</b>	945	3510	1170

9 modules are made of CIGS thin film solar cells and 24 modules are made of monocrystalline silicon solar cells, of which 18 belong to 3 fixed PV systems and 6 to photovoltaic tracker system. Do not forget tracker PV system is out of scope of the project.

Do not forget the performance of a PV-system is given by the output in kWh per installed kW during a given time period. That is why throughout this project, each time a number of photovoltaic systems is named, and it is related to 1 kW. Due to 9 CIGS modules and 6 monocrystalline modules give, respectively, around  $1 \text{ kW}_p$ , they are considered for the performance comparison.

For both kinds of technologies, electrical characteristics are included in Table 3.2 while mechanical specifications are included in Table 3.3.

**Table 3.2. Electrical characteristics for each installed solar cell technology at Standard Test Conditions (STC) and Normal Operating Cell Temperature (NOCT).**

<b>POWER CLASS</b>		<b>[W]</b>	<b>m-Si 195</b>	<b>CIGS 105</b>
<b>PERFORMANCE AT STC (<math>1000 \text{ W/m}^2</math>, <math>25^\circ\text{C}</math>, AM 1.5 G SPECTRUM)</b>				
<b>Rated Maximum Power</b>	<b><math>P_{MPP}</math></b>	<b>[W]</b>	195	105
<b>Short Circuit Current</b>	<b><math>I_{SC}</math></b>	<b>[A]</b>	5.814	1.68
<b>Open Circuit Voltage</b>	<b><math>V_{OC}</math></b>	<b>[V]</b>	45.26	91.6
<b>Current at <math>P_{MPP}</math></b>	<b><math>I_{MPP}</math></b>	<b>[A]</b>	5.383	1.49
<b>Voltage at <math>P_{MPP}</math></b>	<b><math>V_{MPP}</math></b>	<b>[V]</b>	36.52	70.5
<b>Nominal Efficiency</b>	<b><math>\eta</math></b>	<b>[%]</b>	15.27	$\geq 11.2$
<b>PERFORMANCE AT NOCT (<math>800 \text{ W/m}^2</math>, <math>47\pm 3^\circ\text{C}</math> y <math>51\pm 2^\circ\text{C}</math>, AM 1.5 G SPECTRUM)</b>				
<b>Maximum Power</b>	<b><math>P_{MPP}</math></b>	<b>[W]</b>	142	75.9
<b>Short Circuit Current</b>	<b><math>I_{SC}</math></b>	<b>[A]</b>	4.712	1.34
<b>Open Circuit Voltage</b>	<b><math>V_{OC}</math></b>	<b>[V]</b>	40.97	83.4
<b>Current at <math>P_{MPP}</math></b>	<b><math>I_{MPP}</math></b>	<b>[A]</b>	4.33	1.18
<b>Voltage at <math>P_{MPP}</math></b>	<b><math>V_{MPP}</math></b>	<b>[V]</b>	32.80	64
<b>TEMPERATURE COEFFICIENTS (AT <math>1000 \text{ W/m}^2</math>, AM 1.5 G SPECTRUM)</b>				
<b>Temperature Coefficient of <math>I_{SC}</math></b>	<b><math>\alpha</math></b>	<b>[%/<math>^\circ\text{C}</math>]</b>	+0.06	$+0.00\pm 0.04$
<b>Temperature Coefficient of <math>V_{OC}</math></b>	<b><math>\beta</math></b>	<b>[%/<math>^\circ\text{C}</math>]</b>	-0.39	$-0.29\pm 0.04$
<b>Temperature Coefficient of <math>P_{MPP}</math></b>	<b><math>\gamma</math></b>	<b>[%/<math>^\circ\text{C}</math>]</b>	-0.44	$-0.38\pm 0.04$

**Table 3.3. Mechanical specification for each installed solar cell technology**

		<b>m-Si</b>	<b>CIGS</b>
<b>Length</b>	<b>[mm]</b>	1580	1190
<b>Width</b>	<b>[mm]</b>	808	789.5
<b>Thickness</b>	<b>[mm]</b>	35	7.3
<b>Surface area</b>	<b>[m<sup>2</sup>]</b>	1.28	0.94
<b>Weight</b>	<b>[kg]</b>	15	16.5

### 3.1.3. INVERTERS AND MAXIMIZERS

To make it possible to connect the solar panel to the mains voltage is converted by an inverter. The package uses a tried and tested power inverters from small and micro-inverters from AEConversion.

Each solar module, on the other hand, is equipped with its own maximizer. This electronic device is mounted behind the modules on the mounting rails in the rack. The system is electronically and automatically designed for the monitoring of individual modules under maximum power point (MPP) conditions that allow the extraction of the energy yield of different modules under optimum conditions. It can also be used to monitor the performance and long-term stability of modules under realistic field conditions. The monitoring system consists of an individual MPP tracker attached to each module under test. The measurement data are transmitted to a central multichannel data logger by means of analog voltages proportional to the current at MPP, i.e.,  $I_{MPP}$ , and voltage at MPP, i.e.,  $V_{MPP}$ , of the modules, and adapted for the conditions of light and temperature.

### 3.1.4. PYRANOMETERS

A pyranometer is a device used for measuring solar irradiance on a planar surface and it is designed to measure the solar radiation flux density in  $W/m^2$  from the hemisphere above within a wavelength range from 285 nm to 2800 nm.

Two pyranometers placed on the system of the laboratory are installed since 24/03/2016 as is displayed in Fig 3.2. Each one has different functions: the first pyranometer is on horizontal surface giving the horizontal irradiance; the second pyranometer is on the same tilt as PV-modules; and there is an extra measure, named pyranometer number 3, that it gives diffuse irradiance, obtained by the relationship between pyranometers and irradiances according to the following equations:

$$I_{b,n} = \frac{I_h - I_{d,h}}{\cos \theta_z}$$

$$I = I_{b,n} \cdot \cos \theta_z$$

$$\theta_z = 90 - \alpha_s$$

where  $I_{b,n}$  is the beam irradiance in the normal plane,  $I_h$  is the total irradiance in the horizontal plane,  $I_{d,h}$  is the diffuse irradiance in the horizontal plane, and  $\alpha_s$  is the altitude or inclination, defined like the angle between a tilted surface and horizontal plane.

Since pyranometer number 2 has the same tilt as PV modules, it must be used for the comparison between materials. In addition, it gives the highest solar irradiance at 12:00 during sunny days.



*Fig 3.2. Pyranometers number 1 and number 2 placed on the laboratory system.*

### 3.2. PROCEDURE AND OPERATING CONDITIONS

In the laboratory various studies on how shadows affect the electrical performance in the different modules that are installed are made. This project is not intended to study the fill factor. This is the reason why it researches only during clear, sunny days along period of time when shadows are not affecting on the solar cells, from 8:00 to 14:00. In addition, don't forget tracker PV system is also out of scope of the project.

A logger monitors the power production output from the solar cell system and the irradiance from the sun. On one hand, power output data have been registered for each solar cells technology since July 2014 to May 2016 with a time resolution about 10 minutes. On the other hand, installation of pyranometers in the laboratory system was conducted in March 2016, so irradiance data have been registered since 24/03/2016.

In order to analyze the performance of a solar installation, it is necessary to analyze the conversion of electricity from solar cells as a function of solar radiation. This

radiation varies depending on the time of year. The Swedish climate is characterized by cold winters with short days and long summer days where most of the annual solar radiation occurs.

To sum up, the methodology has the next steps:

1. Display of daily PV conversion as a function of time (from 8:00 to 14:00) since July 2014 onwards.
2. Calculation of solar radiation through irradiance per square meter received and ten minutes data. This means, solar radiation must be divided by six because is the data number of 10 minutes per hour.
3. Calculation of PV yield. PV energy output is divided by peak power at STC of each installed PV-system (1.17 kW for silicon and 0.945 kW for CIGS solar cells)
4. Calculation of f ratio, which is defined as the ratio between CIGS and m-Si daily performance.
5. Calculation of effective efficiency ( $\eta_{eff}$ ).
6. Calculation of module performance ratio ( $PR_M$ ), also called capacity factor ( $\phi$ ).

Steps number 5 and 6 can be interchanged since  $PR_M$  also can be obtained like PV yield divided by solar radiation.



## 4. RESULTS

Solar radiation and PV conversion measures and efficiency calculations for single crystal silicon and CIGS modules are reported in this chapter.

Daily measures and calculations of photovoltaic energy output, the sum of global irradiance per square meter received by pyranometer 2 and PV module yield for each solar cells technology per each evaluated month (March, April and May) are displayed in Table 4.1, Table 4.2, Table 4.3, respectively.

**Table 4.1. Daily data and calculations of monocrystalline silicon and CIGS thin film solar cells at NOCT conditions for PV module conversion, global irradiance per square meter received, PV module yield and f ratio: March 2016**

Day	PV conversion [kWh/day]		Solar Radiation [kWh/m <sup>2</sup> -day]	PV yield [kWh/kWp-day]		f [-]
	m-Si	CIGS		m-Si	CIGS	
24-mar	3,47	2,44	3,32	2,97	2,58	0,87
25-mar	0,37	0,25	0,67	0,32	0,26	0,84
26-mar	2,51	1,69	2,43	2,15	1,79	0,83
27-mar	2,84	1,97	2,76	2,43	2,08	0,86
28-mar	4,43	3,08	4,14	3,79	3,26	0,86
29-mar	0,57	0,39	0,83	0,49	0,41	0,85
30-mar	0,85	0,60	1,14	0,73	0,63	0,87
31-mar	2,56	1,76	2,54	2,19	1,86	0,85

In the same way, PV module yield in kWh/kW-day as function of the sum of global irradiance per square meter received per day for each solar cells technology (m-Si and CIGS) is displayed for each evaluated month (March, April and May) according to Fig 4.1, Fig 4.2, and Fig 4.3, respectively.

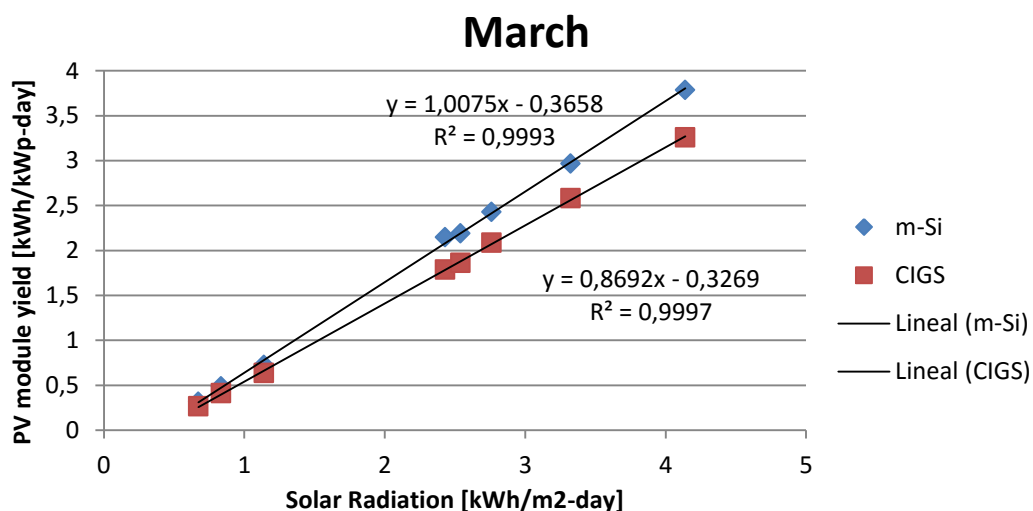


**Fig 4.1. PV module yield as function of solar radiation for each solar cells technology: March 2016**

A nearly linear trend is observed along the month of March for both kinds of technologies. The highest solar radiation value is 4.14 kWh/ m<sup>2</sup>-day and is received during the 28<sup>th</sup> of March where the ratio between CIGS and m-Si is 0.86.

*Table 4.2. Daily data and calculations of monocrystalline silicon and CIGS thin film solar cells at NOCT conditions for PV module conversion, global irradiation per square meter received, PV module yield and f ratio: April 2016*

Day	PV conversion [kWh/day]		Solar Radiation [kWh/m <sup>2</sup> -day] Pyranometer 2	PV yield [kWh/kWp-day]		f [-] CIGS/m-Si
	m-Si	CIGS		m-Si	CIGS	
01-abr	4,18	2,94	4,06	3,57	3,11	0,87
02-abr	0,52	0,37	0,87	0,44	0,39	0,88
03-abr	3,39	2,39	3,37	2,90	2,53	0,87
04-abr	0,33	0,24	0,64	0,28	0,25	0,90
05-abr	0,16	0,08	0,44	0,14	0,08	0,62
06-abr	0,03	0,03	0,13	0,03	0,03	1,24
07-abr	0,23	0,13	0,49	0,20	0,14	0,70
08-abr	1,25	0,91	1,48	1,07	0,96	0,90
09-abr	0,67	0,49	0,99	0,57	0,52	0,91
10-abr	4,52	3,19	4,35	3,86	3,38	0,87
11-abr	3,49	2,45	3,47	2,98	2,59	0,87
12-abr	3,53	2,44	3,43	3,02	2,58	0,86
13-abr	3,14	2,24	3,16	2,68	2,37	0,88
14-abr	4,70	3,36	4,53	4,02	3,56	0,89
15-abr	3,63	2,54	3,51	3,10	2,69	0,87
16-abr	2,96	2,12	3,06	2,53	2,24	0,89
17-abr	0,10	0,05	0,32	0,09	0,05	0,62
18-abr	4,36	3,10	4,24	3,73	3,28	0,88
19-abr	1,40	1,00	1,61	1,20	1,06	0,88
20-abr	5,06	3,57	4,84	4,32	3,78	0,87
21-abr	3,52	2,54	3,64	3,01	2,69	0,89
22-abr	1,50	1,11	1,80	1,28	1,17	0,92
23-abr	0,88	0,66	1,25	0,75	0,70	0,93
24-abr	3,97	2,86	3,96	3,39	3,03	0,89
25-abr	2,09	1,52	2,31	1,79	1,61	0,90
26-abr	4,66	3,29	4,45	3,98	3,48	0,87
27-abr	0,42	0,32	0,79	0,36	0,34	0,94
28-abr	0,28	0,19	0,56	0,24	0,20	0,84
29-abr	1,91	1,43	2,18	1,63	1,51	0,93
30-abr	4,30	3,02	4,15	3,68	3,20	0,87



There are more data for case of April, a nearly linear trend is also observed for both kinds of technologies although the gradient of each line is lower. The highest solar radiation value is 4.53 kWh/ m<sup>2</sup>-day and is received during the 20<sup>th</sup> of April with an f ratio of 0.87. This means the highest PV conversion is for that day, 5.06 kWh/ day for six single-crystal modules and 3.57 kWh/ day for nine CIGS modules.

In spite of this, it can be observed the f ratio is not the highest one. There are some f ratio values between 0.87 and 0.94. The f ratio value during the 6<sup>th</sup> of April is more than the unity so there is a shadow problem this day.

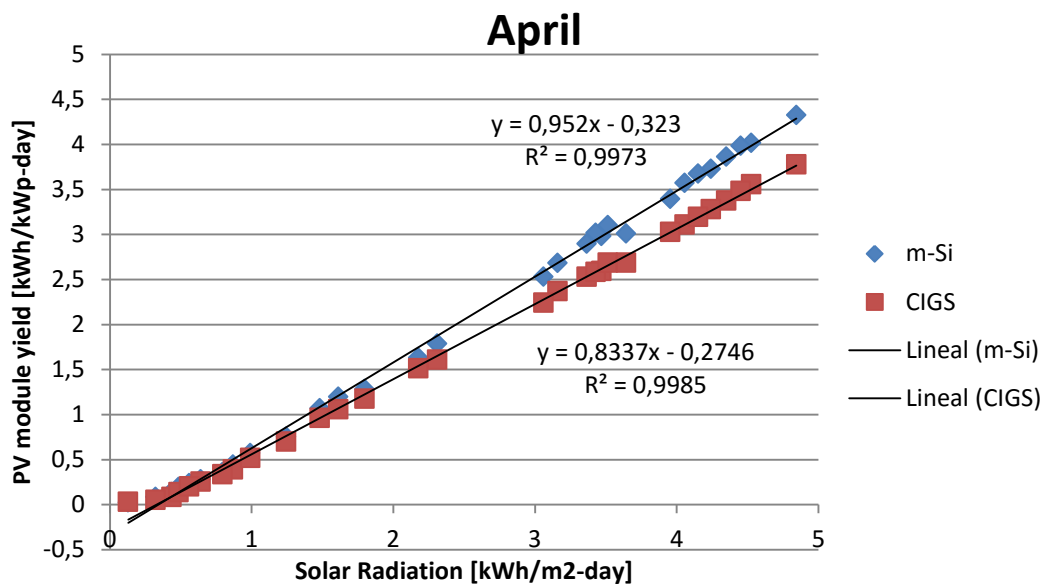


**Fig 4.2. PV module yield as function of solar radiation for each solar cells technology: April 2016**

The PV system made of monocrystalline silicon solar cells was disconnected by means of a cover from 10<sup>th</sup> to 11<sup>th</sup> of May. That is because it was needed for the aim of other research about shadow effect. The PV system was not cleaned until 13<sup>th</sup> of May.

Consequently, no common values could have been obtained from 10<sup>th</sup> to 13<sup>th</sup> of May and could have modified in any way the expected monthly results, reaching wrong considerations or conclusions. That is why these data (highlighted in orange in Table 4.3) have not been represented in Fig 4.3 in order to reach a better fine-tuning parameter.

In case of May, do not keeping in mind uncommon measures, the gradient of each line is similar to April. The highest solar radiation value is 4.94 kWh/ m<sup>2</sup>-day and is received during the 5<sup>th</sup> of May with an f ratio of 0.88. The highest PV conversion is for that day, 4.96 kWh/ day for 6 m-Si modules and 3.51 kWh/ day for 9 CIGS modules. There are some f ratio values bigger than the unity so there are shadow problems these days.

**Table 4.3. Daily data and calculations of monocrystalline silicon and CIGS thin film solar cells at NOCT conditions for PV module conversion, global irradiation per square meter received, PV module yield and f ratio: May 2016**

Day	PV conversion [kWh/day]		Solar Radiation [kWh/m2-day]	PV yield [kWh/kWp-day]		F [-]
	m-Si	CIGS		m-Si	CIGS	
01-may	2,32	1,68	2,53	1,98	1,78	0,90
02-may	4,60	3,28	4,49	3,93	3,47	0,88
03-may	3,89	2,79	4,03	3,32	2,95	0,89
04-may	4,63	3,26	4,63	3,96	3,45	0,87
05-may	4,96	3,51	4,94	4,24	3,71	0,88
06-may	4,61	3,26	4,56	3,94	3,45	0,88
07-may	4,55	3,21	4,61	3,89	3,40	0,87
08-may	4,68	3,30	4,79	4,00	3,49	0,87
09-may	4,20	2,99	4,31	3,59	3,16	0,88
10-may	2,33	3,01	4,42	1,99	3,19	1,60
11-may	1,68	3,38	4,68	1,44	3,58	2,49
12-may	3,36	3,25	4,55	2,87	3,44	1,20
13-may	0,16	0,09	0,41	0,14	0,10	0,70
14-may	0,19	0,09	0,44	0,16	0,10	0,59
15-may	3,38	2,52	3,61	2,89	2,67	0,92
16-may	0,12	0,06	0,37	0,10	0,06	0,62
17-may	1,58	1,18	1,96	1,35	1,25	0,92
18-may	1,64	1,27	2,09	1,40	1,34	0,96
19-may	2,98	2,24	3,30	2,55	2,37	0,93
20-may	4,21	3,05	4,35	3,60	3,23	0,90
21-may	1,65	1,38	2,23	1,41	1,46	1,04
22-may	1,30	1,06	1,83	1,11	1,12	1,01
23-may	3,84	2,90	4,13	3,28	3,07	0,94

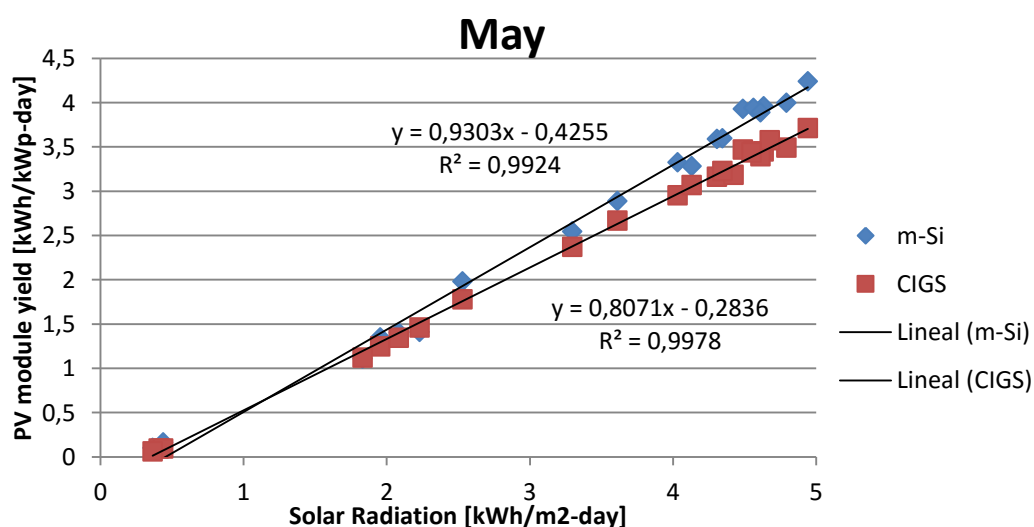


**Fig 4.3. PV module yield as function of solar radiation for each solar cells technology: May 2016.**

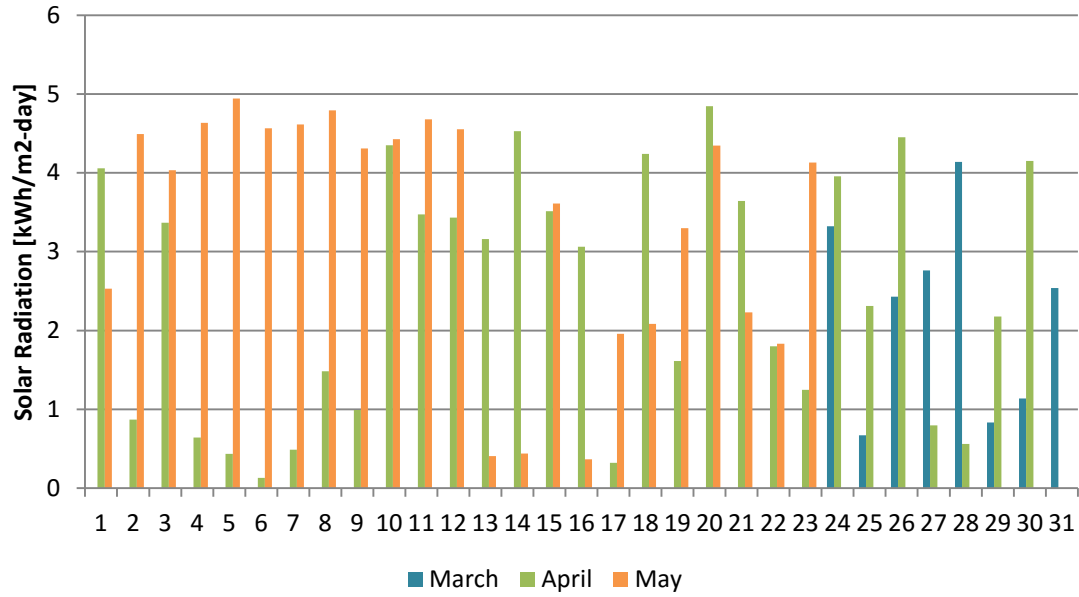


*Fig 4.4. Daily solar radiation for March, April and May.*

To sum up then, the best days regarding solar radiation according to Fig 4.4 for each month are:

- ✓ March 2016: 24<sup>th</sup>, 27<sup>th</sup>, and 28<sup>th</sup>.
- ✓ April 2016: 1<sup>st</sup>, 10<sup>th</sup>, 14<sup>th</sup>, 18<sup>th</sup>, 20<sup>th</sup>, 26<sup>th</sup>, and 30<sup>th</sup>.
- ✓ May 2016: 2<sup>nd</sup>, 4<sup>th</sup>, 5<sup>th</sup>, 6<sup>th</sup>, 7<sup>th</sup>, 8<sup>th</sup>, 20<sup>th</sup>, and 23<sup>rd</sup>.

The best clear sunny days for each month are the 28th of March, the 20th of March and the 5th of May; they are displayed in Fig 4.4.

These three best days of each month are reported as a function of time for the following parameters: energy output or PV conversion output, PV module yield and f ratio, as is displayed in Fig 4.5, Fig 4.6 and Fig 4.7, respectively.

Shadows can be observed in Fig 4.5 (a), since there are some discontinuities inside of interval from 8:00 to 14:00; time when shadows from buildings or staircases, which do not belong to sky, have no effect. The same trend is displayed in Fig 4.6 (a).

On the other hand, it seems that 20<sup>th</sup> of April and 5<sup>th</sup> of May are really good sunny day with no shadow effect according to Fig 4.5 (b) and Fig 4.5 (c). The same trend is displayed in Fig 4.6 (b) and Fig 4.6 (c).

In addition, PV conversion and PV yield diagrams since July 2014 onwards, like Fig 4.5 and Fig 4.6, were presented to the thesis supervisor, off of this report.

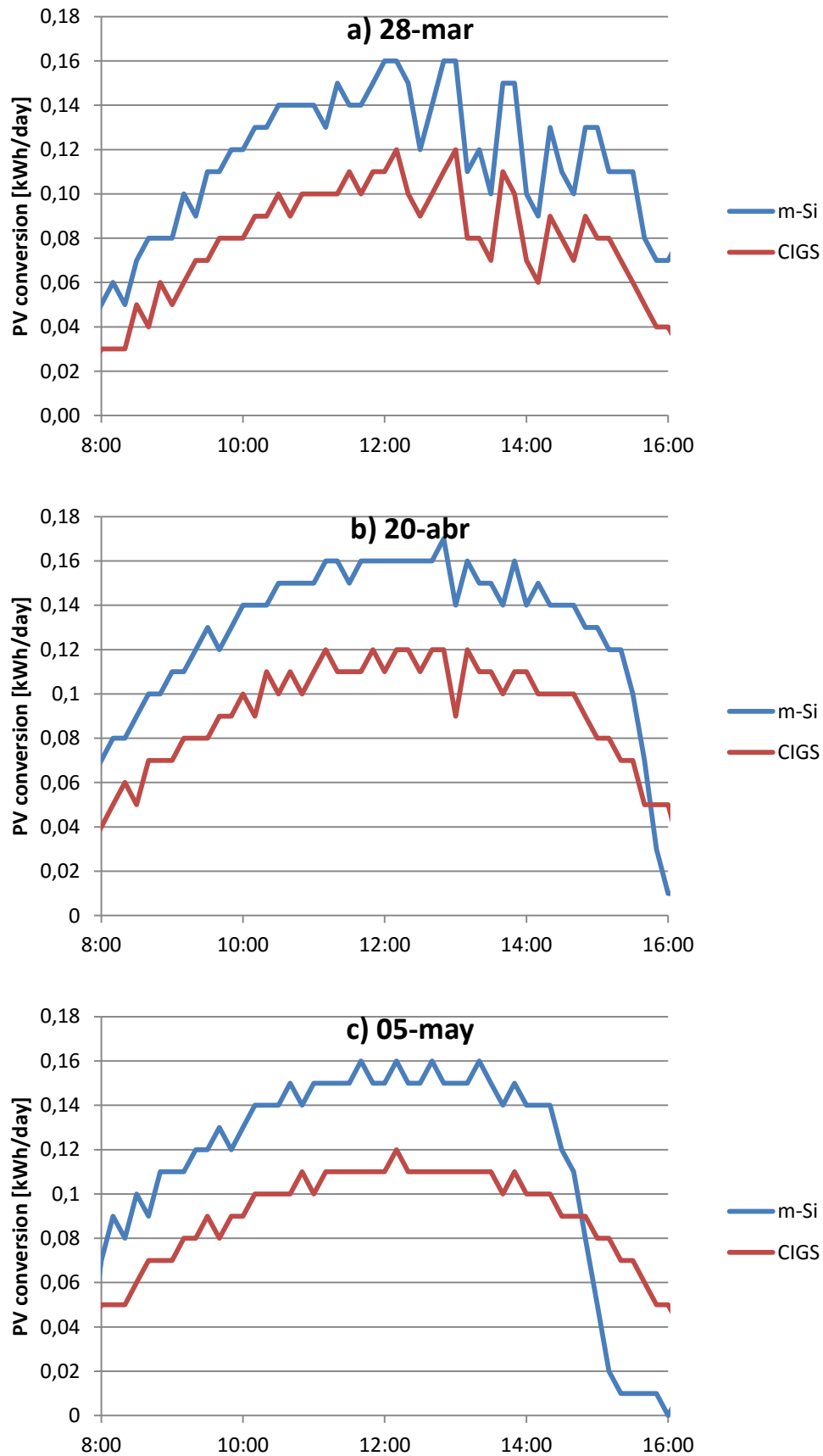


*Fig 4.5. PV conversion as a function of time for each solar cells technology: a) 28/03/2016; b) 20/04/2016; c) 05/05/2016.*

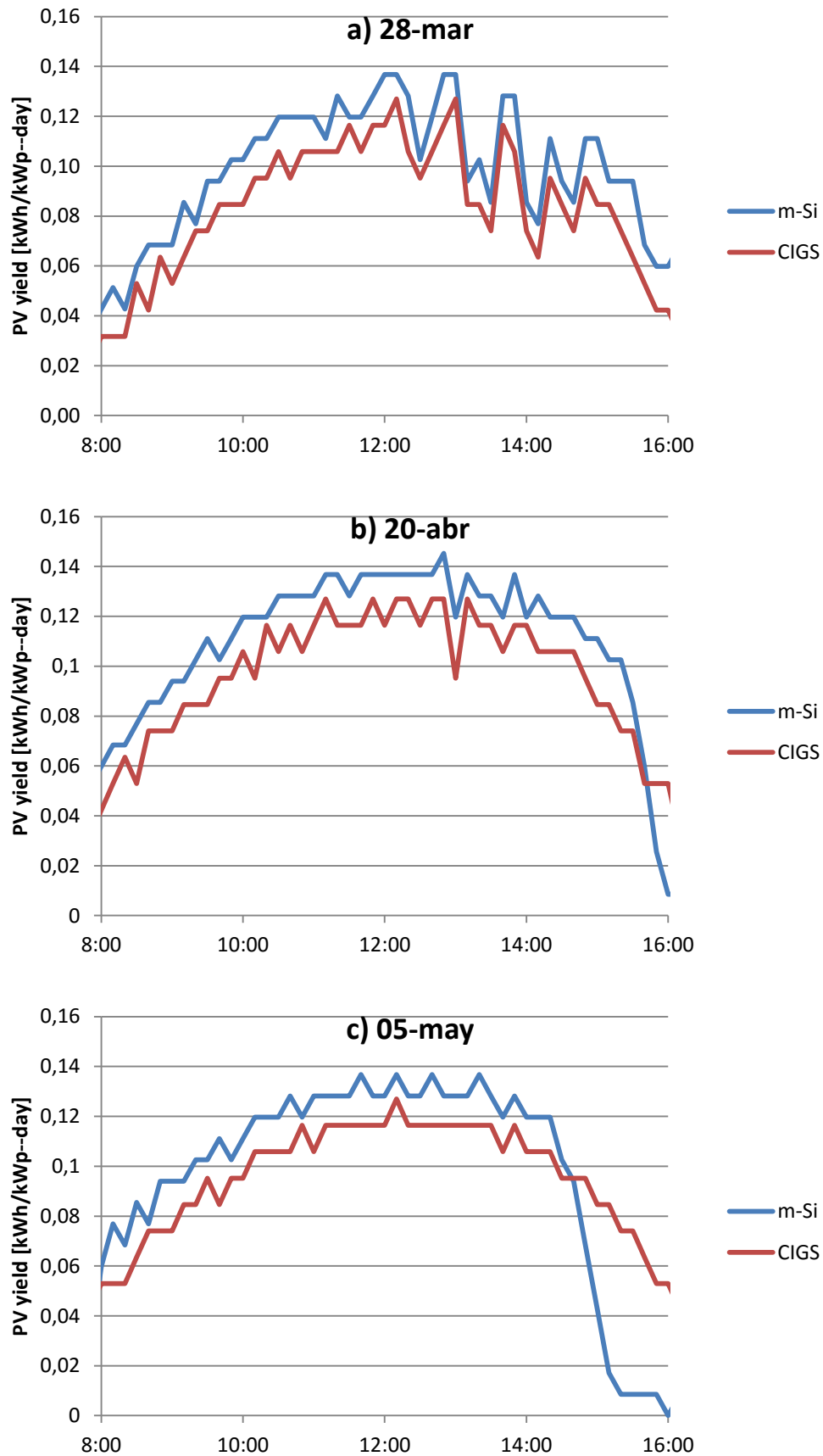


**Fig 4.6.** PV yield as a function of time for each solar cells technology: a) 28/03/2016; b) 20/04/2016; c) 05/05/2016.

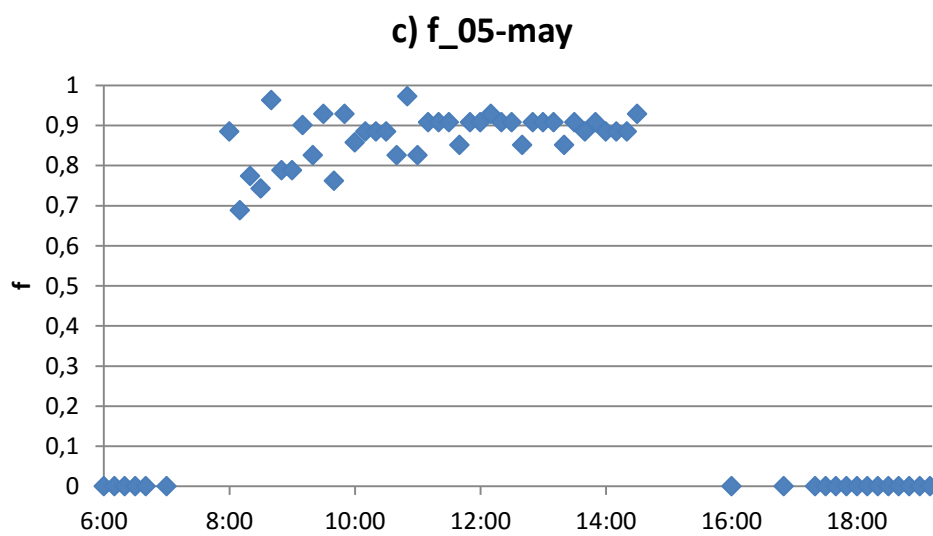
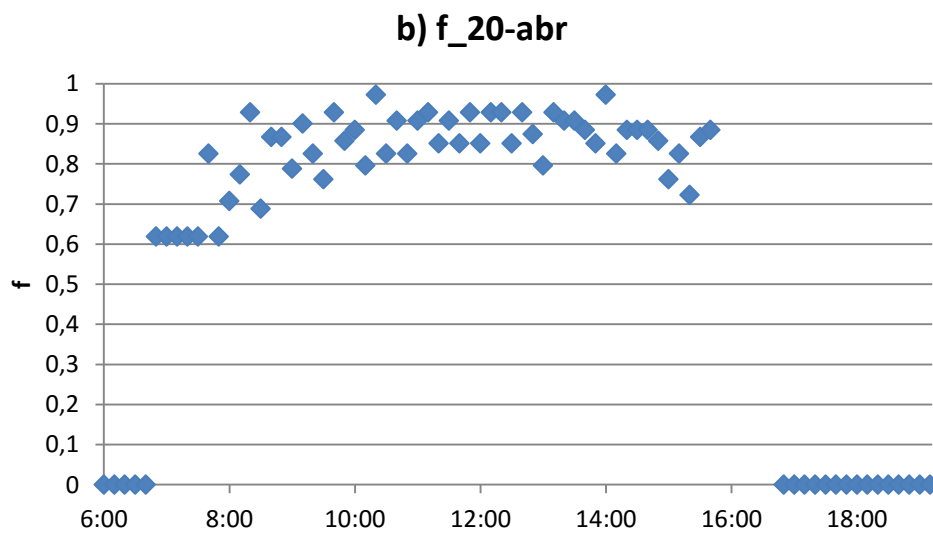
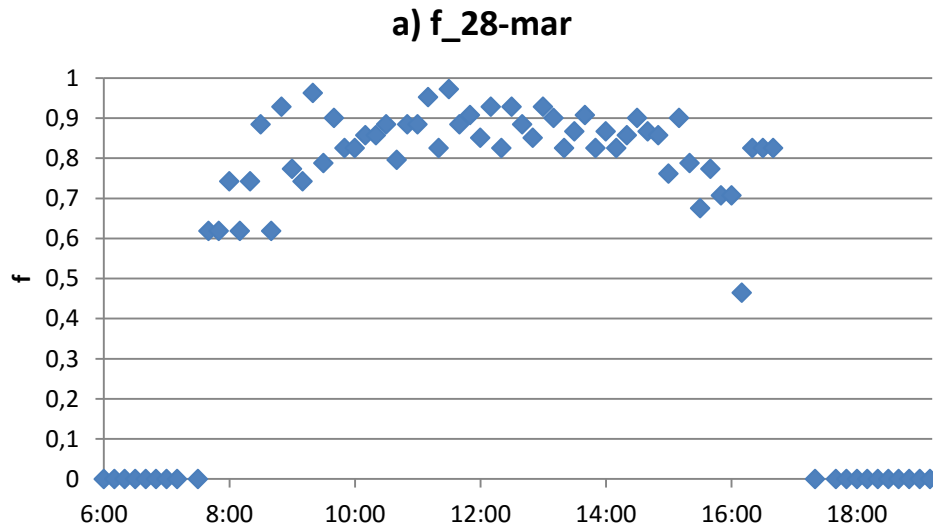


**Fig 4.7. Ratio “f” between CIGS and mono-Si daily performance per  $kW_p$  as a function of time for each solar cells technology: a) 28/03/2016; b) 20/04/2016; c) 05/05/2016**

**Table 4.4. Calculations of effective efficiency and module performance ratio: March 2016**

Day	Solar Radiation [kWh/m <sup>2</sup> -day]	$\eta_{eff}$		PR_M	
		m-Si	CIGS	m-Si	CIGS
24-mar	3,32	13,63%	8,68%	89,27%	77,53%
25-mar	0,67	7,18%	4,40%	47,05%	39,26%
26-mar	2,43	13,49%	8,23%	88,33%	73,46%
27-mar	2,76	13,43%	8,44%	87,95%	75,35%
28-mar	4,14	13,97%	8,80%	91,49%	78,57%
29-mar	0,83	8,93%	5,53%	58,47%	49,41%
30-mar	1,14	9,74%	6,23%	63,79%	55,61%
31-mar	2,54	13,16%	8,20%	86,21%	73,21%

**Table 4.5. Calculations of effective efficiency and module performance ratio: April 2016**

Day	Solar Radiation [kWh/m <sup>2</sup> -day]	$\eta_{eff}$		PR_M	
		m-Si	CIGS	m-Si	CIGS
01-abr	4,06	13,45%	8,57%	88,09%	76,52%
02-abr	0,87	7,81%	5,03%	51,14%	44,94%
03-abr	3,37	13,15%	8,40%	86,10%	74,97%
04-abr	0,64	6,73%	4,43%	44,05%	39,57%
05-abr	0,44	4,78%	2,17%	31,31%	19,33%
06-abr	0,13	3,03%	2,74%	19,83%	24,49%
07-abr	0,49	6,17%	3,16%	40,42%	28,22%
08-abr	1,48	11,02%	7,26%	72,13%	64,86%
09-abr	0,99	8,82%	5,84%	57,77%	52,18%
10-abr	4,35	13,57%	8,67%	88,84%	77,44%
11-abr	3,47	13,13%	8,35%	85,97%	74,54%
12-abr	3,43	13,44%	8,41%	87,99%	75,12%
13-abr	3,16	12,97%	8,38%	84,93%	74,83%
14-abr	4,53	13,55%	8,78%	88,74%	78,36%
15-abr	3,51	13,48%	8,55%	88,30%	76,31%
16-abr	3,06	12,63%	8,19%	82,70%	73,15%
17-abr	0,32	4,04%	1,83%	26,49%	16,36%
18-abr	4,24	13,42%	8,64%	87,88%	77,18%
19-abr	1,61	11,33%	7,33%	74,21%	65,47%
20-abr	4,84	13,64%	8,71%	89,29%	77,81%
21-abr	3,64	12,61%	8,25%	82,61%	73,62%
22-abr	1,80	10,89%	7,30%	71,34%	65,20%
23-abr	1,25	9,23%	6,27%	60,42%	55,97%
24-abr	3,96	13,10%	8,55%	85,80%	76,34%
25-abr	2,31	11,81%	7,78%	77,33%	69,46%
26-abr	4,45	13,67%	8,74%	89,49%	78,04%
27-abr	0,79	6,90%	4,76%	45,17%	42,51%
28-abr	0,56	6,54%	4,02%	42,82%	35,88%
29-abr	2,18	11,45%	7,77%	74,98%	69,33%
30-abr	4,15	13,52%	8,60%	88,53%	76,80%

Effective efficiency and module performance ratio are displayed for March, April, and May, monthly average and best sunny days according to Table 4.4, Table 4.5 and Table 4.6. In the same way, the Mean and the Standard Deviation of these parameters are displayed for the whole month (Table 4.7), for sunny days of each month, highlighted in blue (Table 4.8), and for the best days of each month (Table 4.9).

**Table 4.6. Calculations of effective efficiency and module performance ratio: May 2016**

Day	Solar Radiation [kWh/m <sup>2</sup> -day]	$\eta_{eff}$		PR_M	
		m-Si	CIGS	m-Si	CIGS
01-may	2,53	11,97%	7,85%	78,42%	70,13%
02-may	4,49	13,37%	8,64%	87,59%	77,13%
03-may	4,03	12,59%	8,18%	82,47%	73,06%
04-may	4,63	13,04%	8,32%	85,42%	74,29%
05-may	4,94	13,10%	8,40%	85,79%	74,99%
06-may	4,56	13,19%	8,45%	86,36%	75,42%
07-may	4,61	12,88%	8,23%	84,34%	73,49%
08-may	4,79	12,75%	8,14%	83,48%	72,70%
09-may	4,31	12,73%	8,21%	83,37%	73,30%
10-may	4,42	6,87%	8,05%	45,02%	71,83%
11-may	4,68	4,69%	8,55%	30,71%	76,32%
12-may	4,55	9,64%	8,45%	63,13%	75,41%
13-may	0,41	5,11%	2,61%	33,49%	23,26%
14-may	0,44	5,66%	2,43%	37,04%	21,67%
15-may	3,61	12,22%	8,25%	80,01%	73,68%
16-may	0,37	4,29%	1,94%	28,09%	17,35%
17-may	1,96	10,55%	7,14%	69,07%	63,71%
18-may	2,09	10,27%	7,20%	67,23%	64,30%
19-may	3,30	11,80%	8,04%	77,29%	71,75%
20-may	4,35	12,64%	8,30%	82,80%	74,09%
21-may	2,23	9,66%	7,32%	63,25%	65,33%
22-may	1,83	9,26%	6,84%	60,66%	61,09%
23-may	4,13	12,13%	8,30%	79,46%	74,12%

**Table 4.7. Mean and Standard Deviation values of effective efficiency, performance ratio and f ratio: case of whole month**

	Month	$\eta_{eff}$		PR_M		f
		m-Si	CIGS	m-Si	CIGS	CIGS/m-Si
Mean ( $\mu$ )	March 2016	11,69%	7,31%	76,57%	65,30%	85,28%
	April 2016	10,66%	6,85%	69,82%	61,16%	87,59%
	May 2016	10,45%	7,30%	68,46%	65,15%	95,17%
	Average	<b>10,94%</b>	<b>7,15%</b>	<b>71,62%</b>	<b>63,87%</b>	<b>89,35%</b>
SD ( $\sigma$ )	March 2016	2,65%	1,68%	17,35%	15,03%	
	April 2016	3,35%	2,24%	21,91%	19,97%	
	May 2016	3,04%	2,03%	19,93%	18,10%	
	Average	<b>3,01%</b>	<b>1,98%</b>	<b>19,73%</b>	<b>17,70%</b>	<b>5,17%</b>



*Table 4.8. Mean and Standard Deviation values of effective efficiency, performance ratio and f ratio: case of sunny days (highlighted in blue)*

	Month	$\eta_{eff}$		PR_M		f
		m-Si	CIGS	m-Si	CIGS	CIGS/m-Si
Mean ( $\mu$ )	March 2016	13,68%	8,64%	89,57%	77,15%	86,13%
	April 2016	13,54%	8,67%	88,70%	77,45%	87,32%
	May 2016	12,89%	8,35%	84,41%	74,53%	88,30%
	Average	<b>13,37%</b>	<b>8,55%</b>	<b>87,56%</b>	<b>76,38%</b>	<b>87,25%</b>
SD ( $\sigma$ )	March 2016	0,27%	0,18%	1,79%	1,64%	
	April 2016	0,09%	0,07%	0,59%	0,67%	
	May 2016	0,39%	0,15%	2,53%	1,34%	
	Average	<b>0,25%</b>	<b>0,14%</b>	<b>1,63%</b>	<b>1,22%</b>	<b>1,09%</b>

*Table 4.9. Effective efficiency, performance ratio and f ratio for the best clear sunny days of each month*

Day	$\eta_{eff}$		PR_M		f
	m-Si	CIGS	m-Si	CIGS	CIGS/m-Si
28-mar	13,97%	8,80%	91,49%	78,57%	85,87%
20-abr	13,64%	8,71%	89,29%	77,81%	87,14%
05-may	13,10%	8,40%	85,79%	74,99%	87,40%



## 5. DISCUSSION

Analyses of the results about the influence of the most important parameters have been carried out in this chapter, according to the results obtained from the methodology proposed in the literature review for single crystal silicon and CIGS modules.

First detailed analysis is carried out about the relationship between both kinds of PV systems for the following parameters: PV conversion, PV conversion per kW installed or PV module yield, and f factor under the influence of time and solar radiation.

The first result of this evaluation was the annual solar irradiation measured by pyranometers with an inclination of 45° like both PV systems. These values are compared with PVGIS database [23] in accordance with the same inclination (Table 5.1) and the optimum inclination for long-term Gävle of 42° statistically (Table 5.2) in a direction towards the south.

**Table 5.1. Usual values in Gävle simulated through PVGIS database for a nominal power of the PV system of 1 kW and a 45°-tilt angle: a) Crystalline silicon; b) CIGS**

Fixed system: inclination=45°; orientation=0°			Crystalline Silicon		CIGS	
Month	$H_d$	$H_m$	$E_d$	$E_m$	$E_d$	$E_m$
Jan	0.70	21.8	0.61	19.0	0.61	18.8
Feb	1.88	52.6	1.59	44.6	1.59	44.5
Mar	3.00	93.0	2.45	76.0	2.46	76.4
Apr	4.47	134	3.48	104	3.55	106
May	5.59	173	4.22	131	4.32	134
Jun	5.44	163	4.00	120	4.10	123
Jul	5.27	163	3.85	119	3.94	122
Aug	4.31	133	3.19	98.8	3.26	101
Sep	3.32	99.5	2.55	76.4	2.59	77.6
Oct	1.89	58.5	1.53	47.3	1.53	47.6
Nov	0.96	28.8	0.81	24.3	0.81	24.2
Dec	0.44	13.6	0.38	11.9	0.38	11.7
Yearly average	3.11	94.7	2.39	72.7	2.43	73.9
Total for year		1140		873		887

Ed: Average daily electricity production from the given system (kWh);

Em: Average monthly electricity production from the given system (kWh);

Hd: Average daily sum of global irradiation per square meter received by the modules of the given system (kWh/m<sup>2</sup>);

Hm: Average sum of global irradiation per square meter received by the modules of the given system (kWh/m<sup>2</sup>).

Since daily solar radiation measures (Table 4.1, Table 4.2 and Table 4.3) are between PVGIS database values, it can be stated that measures are consistent with Table 5.1. These measures are also according to Uppsala report [3], whose monthly solar radiation measures during months of March and April 2011 were 145 kWh / m<sup>2</sup>.

*Table 5.2. Usual values in Gävle simulated through PVGIS database for a nominal power of the PV system of 1 kW and a 42°-tilt angle: a) Crystalline silicon; b) CIGS*

Fixed system: inclination=42°; orientation=0°						
Month	Crystalline Silicon				CIGS	
	$H_d$	$H_m$	$E_d$	$E_m$	$E_d$	$E_m$
Jan	0.68	21.1	0.59	18.4	0.59	18.2
Feb	1.84	51.4	1.56	43.6	1.55	43.5
Mar	2.97	92.0	2.43	75.2	2.44	75.6
Apr	4.48	134	3.49	105	3.55	107
May	5.64	175	4.26	132	4.36	135
Jun	5.51	165	4.06	122	4.16	125
Jul	5.33	165	3.89	121	3.98	124
Aug	4.33	134	3.21	99.4	3.28	102
Sep	3.30	98.9	2.53	76.0	2.57	77.2
Oct	1.86	57.5	1.50	46.6	1.51	46.8
Nov	0.93	28.0	0.79	23.7	0.78	23.5
Dec	0.42	13.2	0.37	11.5	0.36	11.3
Yearly average	<b>3.11</b>	<b>94.7</b>	<b>2.39</b>	<b>72.8</b>	<b>2.43</b>	<b>74.0</b>
Total for year		<b>1140</b>		<b>874</b>		<b>888</b>

Higher solar radiation implies higher Silicon PV modules yield PV module yield respect to CIGS modules. Daily PV conversion measures (Table 4.1, Table 4.2 and Table 4.3) are also consistent with PVGIS database (Table 5.1). A linear trend is observed for both kinds of technologies with respect to solar radiation according to Fig 4.1, Fig 4.2 and Fig 4.3. These parameters as a function of time follow a similar trend than normal distribution of Gauss Seidel according to Fig 4.5 and Fig 4.6.

For the same solar irradiation, no shadowing effect and a basis per kW installed (PV yield), m-Si modules are able to convert more energy than thin film CIGS modules as can be observed comparing Fig 4.6 (a), Fig 4.6 (b) and Fig 4.6 (c).

The highest solar radiation period along a day is around 12:00 during a clear sunny day as the same time as is produced the best PV conversion (Fig 4.5) and PV module yield (Fig 4.6). PV conversion and PV yield curves keep the same trend along a day that can be observed with f ratio (Fig 4.7). About 0.87-0.91 is a common f ratio value during a clear sunny day, when shadows do not affect, according to this report (Table 4.1, Table 4.2, Table 4.3 and Table 4.7) and Uppsala report (Table 2.4) whose f ratio is equal to 0.91.

However, f ratio also varies slightly as a function of time so it comes to a conclusion that does not only depend on shadows and solar radiation; it also depends on incidence angle and operating cell temperature. This can also be observed comparing Table 5.1 and Table 5.2 each other.

Besides, larger daily periods with high solar radiation values and no shadow effect produce a smaller deviation on  $f$  ratio values. These periods are during summertime but this trend can be observed in Fig 4.7 (c) with respect to Fig 4.7 (a), belonging to May 2016 and March 2016, respectively.

From now onwards, second detailed analysis is carried out about calculated effective efficiency at NOCT with respect to nominal efficiency at STC; that is PV module's performance ratio analysis for both technology kinds.

In general terms, effective efficiency and performance ratio of single crystal silicon modules are greater than thin film CIGS ones, both for entire month case as for sunny days case, with which is focused this report. Both trends can be observed in Table 4.7 and Table 4.8, respectively, where monthly average and SD are displayed of these parameters; in Table 4.9 where the best sunny days are displayed; and in Table 4.4, Table 4.5 and Table 4.6 regarding the best values of solar radiation or global irradiation.

For case of sunny days when shadows have no effect, effective efficiency has a mean of 13.37 % and a SD of 0.25% for single crystal silicon PV-system and a mean of 8.55% and a SD of 0.14% for CIGS PV-system. On the other hand, PV module's performance ratio has a mean of 87.56% and a SD of 1.63% for monocrystalline modules and a mean of 76.38% and a SD of 1.22% for thin film CIGS modules. However, both parameters decrease for each month as is displayed in Table 4.8. That is because the mean ambient temperature and the number of sun hour's increase and, thus, normal operating cell temperature has an impact on these parameters.

Despite efficiency at STC for both technology kinds are higher compared to efficiencies at STC provided by Table 2.5; effective efficiency and performance ratio for both technology kinds during a whole month (Table 4.6) are lower than reviewed data, with the exception of monocrystalline silicon effective efficiency for sunny days which is higher (13.37%). Since there are no great differences between these two localizations and between two incidence angles in Table 2.5, the reason because these two parameters are lower could be due to a short time period of measures and do not measured during summertime.

Last hypothesis could be met by means of an assessment along a year and could be compared to Fig 2.16, since lots of PV panels have a specific yield ( $PR_M$ ) between 80 % and 90 %, very close to case of sunny days (87.56 %  $\pm$  1.63 % for m-Si and 76.38%  $\pm$  1.22% for CIGS).

Accordingly, the second analysis comes to the conclusion that single crystal silicon modules present better behavior with respect to energy conversion since effective efficiency and PV module's performance ratio are higher than thin film CIGS ones under field condition.



## 6. CONCLUSIONS

This report has been performed in order to contribute to research on photovoltaic field. The main objective of this project was to evaluate the performance of two different types of solar cells in an outdoor facility in the Swedish climate, particularly on monocrystalline silicon and thin film CIGS solar cells.

All types of thin film CIGS solar cells have reached so far the highest efficiency and therefore are considered to have the best potential in the market. By the other side, Silicon technology has a head-start on owning the highest solar cell and module performance lab values.

In this context, a comparative analysis has been carried out since July 2014, taking into consideration the following aspects:

- ✓ Only clear sunny days have been considered.
- ✓ Fill factor equal to 1. No shadows are considered. This implies that evaluation along a day has been carried out from 8:00 to 14:00.
- ✓ Pyranometers were installed in March 2016, limiting the analysis at this time.
- ✓ Single crystal measures are not common values from 10/05/2016 up to 13/05/2016 due a cover was installed in order to reach the aim of other project performed as the same time.

Throughout two analyses, one comes to the following conclusions on the behavior of the PV systems:

- For both PV systems, overall:
  1. PV module yields depend nearly linearly on solar radiation at given location and tilt for all kinds of technology.
  2. Larger daily periods with high solar radiation values and no shadow effect produce a smaller deviation for f ratio values.
  3. Effective efficiency and PV module's performance ratio depend only slightly on the specific location or tilt angle of the module as long as the average solar radiation remains the same.
  4. At the same time that the ambient temperature and normal operating cell temperature are increased; the mean of the effective efficiency and the performance ratio is slightly smaller.
  5. For case of clear sunny days with respect to the case of a whole month, the mean of the effective efficiency and the performance ratio is increased while the SD is reduced.

➤ PV systems comparison:

6. Higher solar radiation implies single crystal silicon modules have higher PV yield respect to thin film CIGS modules.
7. For the same solar irradiation, no shadowing effect and a basis per kW installed (PV yield), single crystal silicon modules are able to convert more energy than thin film CIGS ones.
8. Single crystal silicon modules present better behavior with respect to energy conversion since effective efficiency is higher than thin film CIGS ones.
9. Single crystal silicon modules under Normal Operating Cell Temperature conditions (NOCT) present a better behavior than thin film CIGS modules with respect to values at Standard Test Conditions (STC) considering that PV module's performance ratio is higher.

The results come to conclude that single crystal silicon modules present a better behavior with respect to energy conversion under no shadows effect conditions by two reason: (1) f ratio is about 87.25% with some variations along a day due to ambient temperature, cell temperature and incidence angle; (2) PV module's performance ratio of monocrystalline silicon modules is higher than thin film CIGS ones during a sunny day about 87.56% and 76.38%, respectively.

In light of the outcome, one can conclude that main goal of project and its scope have been managed to successfully. Measurements of these modules will continue even after the completion of the project and will form a basis for a more detailed analysis in the future.

To confirm these conclusions, it intends to launch a project with the objective of evaluating the data collected and compare the performance of the module after a year of measurements outdoors by the PV module's performance ratio procedure.

Along the same lines, University of Gävle intends to launch a project with the objective of evaluating the potential to be self-sufficient.



## 7. REFERENCES

- [1] R. Elleuch, R. Salhi, J.-L. Deschanvres, and R. Maalej, "Antireflective downconversion ZnO:Er<sup>3+</sup>,Yb<sup>3+</sup> thin film for Si solar cell applications," *J. Appl. Phys.*, vol. 117, no. 5, p. 055301, Feb. 2015.
- [2] Z. Khalid, "What PV Solar Solutions entail for you?," *Dunya Blog*, 14-May-2016. .
- [3] "Mätanläggning för utomhusmätningar på solcellsmoduler i Uppsala - SolElProgrammet." [Online]. Available: <http://www.solelprogrammet.se/Verksamhet/Arkiv1/Rapporter/Matanlaggning-for-utomhusmatningar-pa-solcellsmoduler-i-Uppsala/>. [Accessed: 02-Jun-2016].
- [4] M. Topi, K. Brecl, and J. Sites, "Effective efficiency of PV modules under field conditions," *Prog. Photovolt. Res. Appl.*, vol. 15, no. 1, pp. 19–26, Jan. 2007.
- [5] "TECHNOLOGY | Ubiquitous Energy, Inc." .
- [6] J. A. Duffie and W. A. Beckman, *Solar Engineering of Thermal Processes*. John Wiley & Sons, 2013.
- [7] Spie, "Journal article traces dramatic advances in solar efficiency," *SPIE Newsroom*, Nov. 2015.
- [8] "Solar cell," *Wikipedia, the free encyclopedia*. 21-May-2016.
- [9] mzentgraad, "Photovoltaics Report (Slides) — Fraunhofer ISE." [Online]. Available: <https://www.ise.fraunhofer.de/en/downloads-englisch/pdf-files-englisch/photovoltaics-report-slides.pdf/view>. [Accessed: 02-Jun-2016].
- [10] L. Sang, M. Liao, Y. Koide, and M. Sumiya, "InGa<sub>N</sub>-based thin film solar cells: Epitaxy, structural design, and photovoltaic properties," *J. Appl. Phys.*, vol. 117, no. 10, p. 105706, Mar. 2015.
- [11] D. Hauschild, F. Meyer, S. Pohlner, R. Lechner, R. Dietmüller, J. Palm, C. Heske, L. Weinhardt, and F. Reinert, "Impact of environmental conditions on the chemical surface properties of Cu(In,Ga)(S,Se)<sub>2</sub> thin-film solar cell absorbers," *J. Appl. Phys.*, vol. 115, no. 18, p. 183707, May 2014.
- [12] A. G. Aberle, "Thin-film solar cells," *Thin Solid Films*, vol. 517, no. 17, pp. 4706–4710, Jul. 2009.
- [13] A. V. Shah, R. Platz, and H. Keppner, "Thin-film silicon solar cells: A review and selected trends," *Sol. Energy Mater. Sol. Cells*, vol. 38, no. 1–4, pp. 501–520, 1995.
- [14] J. Pearce and A. Lau, "Net Energy Analysis for Sustainable Energy Production From Silicon Based Solar Cells," pp. 181–186, Jan. 2002.
- [15] "Solar cell efficiency," *Wikipedia, the free encyclopedia*. 30-May-2016.
- [16] S. Rühle, "Tabulated values of the Shockley–Queisser limit for single junction solar cells," *Sol. Energy*, vol. 130, pp. 139–147, Jun. 2016.
- [17] W. Shockley and H. J. Queisser, "Detailed Balance Limit of Efficiency of p-n Junction Solar Cells," *J. Appl. Phys.*, vol. 32, no. 3, pp. 510–519, Mar. 1961.
- [18] Tiedje, E. Yablonovitch, G. D. Cody, and B. G. Brooks, "Limiting Efficiency of Silicon Solar Cells," *IEEE Trans. ELECTRON DEVICES*, vol. ED-31, 1984.
- [19] A. D. Vos, "Detailed balance limit of the efficiency of tandem solar cells," *J. Phys. Appl. Phys.*, vol. 13, no. 5, p. 839, 1980.

- [20] M. A. Green, K. Emery, Y. Hishikawa, W. Warta, and E. D. Dunlop, "Solar cell efficiency tables (Version 45)," *Prog. Photovolt. Res. Appl.*, vol. 23, no. 1, pp. 1–9, Jan. 2015.
- [21] M. A. Green, K. Emery, Y. Hishikawa, W. Warta, and E. D. Dunlop, "Solar cell efficiency tables (version 47)," *Prog. Photovolt. Res. Appl.*, vol. 24, no. 1, pp. 3–11, Jan. 2016.
- [22] "NREL: National Center for Photovoltaics Home Page." [Online]. Available: <http://www.nrel.gov/ncpv/>. [Accessed: 03-Jun-2016].
- [23] "JRC's Institute for Energy and Transport - PVGIS - European Commission." [Online]. Available: <http://re.jrc.ec.europa.eu/pvgis/>. [Accessed: 06-Jun-2016].

